

UNCLASSIFIED

AD NUMBER: AD0436675

LIMITATION CHANGES

TO:

Approved for public release; distribution is unlimited.

FROM:

Distribution authorized to U.S. Government agencies and their contractors; Foreign Government Information; Apr 1963. Other requests shall be referred to Advisory Group for Aeronautical Research and Development, Paris, France.

AUTHORITY

AGARD ltr dtd 8 Jul 1970

UNCLASSIFIED

436675

AD

DEFENSE DOCUMENTATION CENTER

FOR

SCIENTIFIC AND TECHNICAL INFORMATION

CAMERON STATION, ALEXANDRIA, VIRGINIA



UNCLASSIFIED

NOTICE: When government or other drawings, specifications or other data are used for any purpose other than in connection with a definitely related government procurement operation, the U. S. Government thereby incurs no responsibility, nor any obligation whatsoever; and the fact that the Government may have formulated, furnished, or in any way supplied the said drawings, specifications, or other data is not to be regarded by implication or otherwise as in any manner licensing the holder or any other person or corporation, or conveying any rights or permission to manufacture, use or sell any patented invention that may in any way be related thereto.

436675

REPORT 456

ADVISORY GROUP FOR AERONAUTICAL RESEARCH AND DEVELOPMENT

64 RUE DE VARENNE, PARIS VII

REPORT 456

**MEASUREMENTS OF THE CORRELATION
BETWEEN THE FLUCTUATING VELOCITIES
AND THE FLUCTUATING WALL
PRESSURE IN A THICK TURBULENT
BOUNDARY LAYER**

by

W. W. WILLMARTH and C. E. WOOLDRIDGE

APRIL 1963



NORTH ATLANTIC TREATY ORGANIZATION

CATALOGED BY DDC 436675 REPORT 456

AS AD No. _____

DDC
APR 27 1964

NO OTS

NORTH ATLANTIC TREATY ORGANIZATION
ADVISORY GROUP FOR AERONAUTICAL RESEARCH AND DEVELOPMENT

MEASUREMENTS OF THE CORRELATION BETWEEN THE FLUCTUATING
VELOCITIES AND THE FLUCTUATING WALL PRESSURE IN A
THICK TURBULENT BOUNDARY LAYER

by

W.W. Willmarth and C.E. Wooldridge

This Report is one in the Series 448-469 inclusive, presenting papers, with discussions, given at the AGARD Specialists' Meeting on 'The Mechanism of Noise Generation in Turbulent Flow' at the Training Center for Experimental Aerodynamics, Rhode-Saint-Genèse, Belgium, 1-5 April 1963, sponsored by the AGARD Fluid Dynamics Panel

SUMMARY

Turbulent motion in a thick (5 inch) boundary layer with zero longitudinal pressure gradient which is produced by natural transition on a smooth surface has been studied. Measurements have been made of the space-time correlation between the fluctuating wall pressure and the fluctuating velocities in the layer, and between the fluctuating wall pressure and the time derivative of the fluctuating velocity normal to the wall.

At any height in the boundary layer, the velocity disturbance which was correlated with the wall pressure disturbances was convected at the local mean speed. The correlation of the wall pressure with the longitudinal velocity was opposite in sign to the correlation of the wall pressure with the velocity normal to the wall. This implies that the part of the velocity field which is correlated with the wall pressure also produces turbulent shear.

The approximate structure of the pressure velocity correlation was obtained from measurements of the space-time correlation between the wall pressure and the fluctuating velocity at various points in the layer. Isocorrelation contours with zero time delay were mapped in three orthogonal planes parallel and perpendicular to the wall. The structure of the isocorrelation contours suggests that the wall pressure is produced by a hierarchy of eddies which produce turbulent shear and have a greater extent in the stream direction than normal to the stream. In planes parallel to the wall, the contours of the correlation between the wall pressure and velocity normal to the wall exhibit a definite swept-back structure. Farther from the wall, the swept-back structure disappears and the isocorrelation contours are symmetric about a line parallel to the wall and normal to the stream.

532.526.4

3b2f

SOMMAIRE

On a étudié le mouvement turbulent dans une couche limitrophe épaisse (12,7 cm) avec pente de pression longitudinale zéro qui est produite par transition naturelle sur une surface lisse. On a relevé des mesures de la corrélation espace-temps entre la pression de paroi variable et les vitesses variables dans la couche, et entre la pression de paroi variable et la dérivée de temps de la vitesse variable perpendiculaire à la paroi.

A toute hauteur quelconque dans la couche limitrophe, la perturbation de vitesse qui était en corrélation avec les perturbations de pression à la paroi était convectée à la vitesse moyenne locale. La corrélation entre la pression à la paroi et la vitesse longitudinale était de signe opposé à la corrélation entre la pression à la paroi et la vitesse perpendiculaire à la paroi. Ceci implique que la partie du champ de vitesse qui est en corrélation avec la pression à la paroi produit également un cisaillement turbulent.

La structure approximative de la corrélation de vitesse de pression a été obtenue d'après des mesures de la corrélation espace-temps entre la pression à la paroi et la vitesse variable en divers points de la couche. On a tracé des contours d'isocorrélation avec décalage de temps zéro dans trois plans orthogonaux parallèles et perpendiculaires à la paroi. La structure des contours d'isocorrélation tend à montrer que la pression à la paroi résulte d'une hiérarchie de tourbillons qui provoquent un cisaillement turbulent et ont une ampleur plus grande dans le sens du courant que dans le sens perpendiculaire à celui-ci. Dans des plans parallèles à la paroi, les contours de la corrélation entre la pression à la paroi et la vitesse perpendiculaire à la paroi présentent une structure nettement en flèche. En un point plus éloigné de la paroi, la structure en flèche disparaît et les contours d'isocorrélation sont symétriques de part et d'autre d'une ligne parallèle à la paroi et perpendiculaire au courant.

532.526.4

3b2f

CONTENTS

	Page
SUMMARY	ii
SOMMAIRE	iii
LIST OF FIGURES	vi
NOTATION	viii
1. INTRODUCTION	1
2. EXPERIMENTAL APPARATUS AND PROCEDURE	2
2.1 Wind Tunnel Facility	2
2.2 Instrumentation	3
3. EXPERIMENTAL ENVIRONMENT	4
3.1 Extraneous Disturbances	4
3.2 Properties of the Turbulent Boundary Layer used in the Investigation	5
3.2.1 Mean Velocity Profiles	5
3.2.2 Wall Pressure Spectrum	6
3.2.3 Velocity Intensity Profiles	7
3.2.4 Velocity Spectra	7
4. EXPERIMENTAL MEASUREMENTS	9
4.1 Measurements of the Correlations \overline{pu} and \overline{pv}	9
4.2 Measurements of the Correlation $\overline{pv_x}$	11
4.3 Influence of External Disturbances on the Pressure-Velocity Correlations	13
5. QUALITATIVE COMPARISON OF KRAICHNAN'S WALL PRESSURE THEORY WITH THE EXPERIMENTAL RESULTS	15
5.1 A Brief Outline of the Theory for the Wall Pressure	16
5.2 Qualitative Comparison of the Wall Pressure Produced by Interaction of the Turbulence and Mean Shear	18
5.3 Qualitative Discussion of the Turbulence Structure Near the Wall	19
5.4 Discussion of the Effect of Turbulence-Turbulence Interaction Terms on the Wall Pressure	19
6. CONCLUSIONS	20
7. ACKNOWLEDGEMENTS	21
REFERENCES	22

	Page
FIGURES	24
APPENDIX	59
DISCUSSION	61
DISTRIBUTION	

LIST OF FIGURES

		Page
Fig.1	Scale drawing of wind tunnel test section and massive vibration isolation mounting for the transducers	24
Fig.2	Pressure transducer and hot wire installation	25
Fig.3	Mean velocity profiles in the turbulent boundary layer. Refer to Table on page 6 for other boundary layer parameters	26
Fig.4	Dimensionless power spectrum of the wall pressure	27
Fig.5	Turbulent velocity intensity profiles in the frequency band used in the subsequent experiments	28
Fig.6	Intensity profile of longitudinal derivative of velocity normal to wall	28
Fig.7	Dimensionless normalized power spectra of the longitudinal velocity components at various heights in the boundary layer	29
Fig.8	Dimensionless normalized power spectra of the velocity components normal to the wall at various heights in the boundary layer	30
Fig.9-26	Measured values of the space-time correlation of fluctuating velocity with fluctuating wall pressure	31-43
Fig.27	Measured values of the spatial correlation of fluctuating longitudinal velocity with fluctuating wall pressure showing symmetry in the transverse direction	44
Fig.28	Measured values of the space-time correlations of fluctuating transverse velocity with fluctuating wall pressure showing the effect of extraneous large-scale flow disturbance probably caused by Taylor-Goertler vortices and density stratification	44
Fig.29-31	Measured values of the space-time correlation of the time derivative of fluctuating velocity normal to the wall with fluctuating wall pressure	45-46
Fig.32	Correlation contours of R'_{pu} in the x_1 - x_2 plane	47
Fig.33	Correlation contours of R'_{pu} in the x_2 - x_3 plane	48
Fig.34	Correlation contours of R'_{pu} in the x_1 - x_3 plane	49
Fig.35	Correlation contours of R'_{pv} in the x_1 - x_2 plane	50

	Page
Fig.36 Correlation contours of R'_{pv} in the x_2-x_3 plane	51
Fig.37 Correlation contours of R'_{pv} in the x_1-x_3 plane	52
Fig.38 Correlation contours of R'_{pv} in the x_1-x_2 plane	53
Fig.39 Correlation contours of R'_{pv} in the x_2-x_3 plane	54
Fig.40 Correlation contours of R'_{pv} in the x_1-x_3 plane	54
Fig.41 Vector field of correlation	55
Fig.42 Dimensionless power spectrum of the wall pressure measured by four different size transducers	56
Fig.43 Dimensionless root-mean-square wall pressure computed from area under faired curves of Figure 42	57

NOTATION

$E_p(\omega)$	power spectrum of wall pressure
$E_u(\omega)$	power spectrum of longitudinal velocity fluctuation
$E_v(\omega)$	power spectrum of velocity fluctuation normal to plate
d	diameter of sensitive area of transducer
f	frequency
k	wave number; $k = \frac{\omega}{U}$
p'	pressure, mean plus fluctuating
p	fluctuating pressure
R	Reynolds number based on distance from virtual origin of turbulent boundary layer
R_θ	Reynolds number based on momentum thickness
R_{pu}, R_{pv}, R_{pw}	normalized wall pressure-velocity correlations; see Equations (4) and (5)
$R_{p\dot{v}}$	normalized correlation of wall pressure with time derivative of velocity normal to wall, see Equation (9)
R_{pv_x}	normalized correlation of wall pressure with longitudinal spatial derivative of velocity normal to wall; see Equation (8)
$R'_{pu}, R'_{pv}, R'_{pw}$	standardized correlations normalized on velocity field at $y/\delta^* = 0.51$
R_{pp}	normalized wall pressure correlation
R_{uu}, R_{vv}	normalized velocity-velocity correlations
U	mean velocity in boundary layer in stream direction
U_∞	free-stream velocity
U_τ	wall friction velocity
U_c	convection speed of fluctuating velocity field which is correlated with fluctuating wall pressure
u'_i	total velocity components mean plus fluctuating ($i = 1, 2, 3$)

u_i or u, v, w	fluctuating velocities in x, y, z directions ($i = 1, 2, 3$)
\dot{v}	time derivative of velocity fluctuation normal to wall
v_x	longitudinal spatial derivative of velocity fluctuation normal to wall
x_1, x_2, x_3	spatial separations of pressure and velocity transducers in x, y, z directions or x, y, z coordinates
x	distance parallel to wall, increasing in stream direction
y	distance normal to wall, increasing away from wall
z	distance parallel to wall and perpendicular to stream, forming a right-hand Cartesian coordinate system with x and y
δ	boundary layer thickness
δ^*	boundary layer displacement thickness
θ	boundary layer momentum thickness
ν	kinematic viscosity
ρ	density
τ	time delay
τ'	time delay equal to transducer spacing divided by local speed
τ_w	wall shear stress
ω	circular frequency ($= 2\pi f$)
$\overline{(\quad)}$	time average

**MEASUREMENTS OF THE CORRELATION BETWEEN THE FLUCTUATING
VELOCITIES AND THE FLUCTUATING WALL PRESSURE
IN A THICK TURBULENT BOUNDARY LAYER**

W.W. Willmarth* and C.E. Wooldridge**

1. INTRODUCTION

This Report is concerned with the relationship between the turbulent velocity field and the pressure fluctuations produced at the wall beneath a thick turbulent boundary layer. Previous experimental investigations of the structure of the turbulence in the boundary layer have considered separately either the fluctuating velocity field or the fluctuating wall pressure. By consideration of the relationship between the fluctuating velocity field and the wall pressure, additional information about the structure of turbulence in the boundary layer is obtained. We also are able to qualitatively relate our measurements to the approximate, linearized theory for the wall pressure fluctuations put forward by Kraichnan¹.

The background for new investigations of the structure of turbulent shear flow are the extensive investigations of the turbulent velocity field made first by Townsend² and later by Schubauer and Klebanoff³, Laufer⁴, Klebanoff⁵, and Corsin and Kistler⁶. Most of our knowledge about the structure of turbulence in a shear flow rests on their measurements of spatial correlations between turbulent velocities and power spectra of turbulent velocity components. A new development was initiated by Favre, Gaviglio, and Dumas⁷ who were the first to measure spatial correlations with variable time delay obtained with a tape recorder. The introduction of time delay made it possible to study the evolution of turbulent eddies. Previously, this had been possible only in the turbulence field downstream of a grid where turbulent decay was the important feature of the problem, and spatial correlations, with the aid of Taylor's hypothesis, suffice for a study of the evolution (decay) of grid turbulence. Favre, et alii, measured space-time correlations of the streamwise fluctuating velocity component in the boundary layer and were able to determine the range of validity of Taylor's hypothesis and the evolution of velocity correlations as eddies are carried downstream. They found that at a certain optimum time delay, for any given streamwise separation between two hot wires, a maximum of the correlation was obtained when one wire, directly downstream of the other was moved normal to the wall. The lines connecting points of maximum correlation at optimum time delay were inclined away from the surface making an angle of approximately 2° with the stream lines.

Later, Grant⁸ reported measurements of the spatial correlations of each of the three components of the fluctuating velocity in the boundary layer. Grant found evidence of jet-like stress relieving motions which move outward and downstream. He suggested that the lines of maximum correlation found by Favre and his collaborators are caused by the jet-like stress relieving motions.

* Professor, Department of Aeronautical and Astronautical Engineering, College of Engineering, The University of Michigan, Ann Arbor, Michigan, U.S.A.

** Research Engineer, United Technology Corporation, Sunnyvale, California, U.S.A.

In the past few years, numerous investigations of the correlations and spectra of wall pressure fluctuations have been reported. The most recent investigations were made by Bull⁹, Corcos¹⁰, and Willmarth and Wooldridge¹¹. The general features of the structure of the wall pressure correlation field in space and time are quite well documented. The wall pressure fluctuations are produced by convected turbulent eddies with apparent convection velocities varying from $0.56 U_\infty$ when the measuring points are separated by a small distance in the stream direction to $0.83 U_\infty$ when the streamwise separation between measuring points is large. This behavior of the wall pressure field is probably caused by the generation and decay of small scale eddies near the wall where the velocity is low and by the large scale eddies and jet-like stress relieving motions farther from the wall.

The details of the structure of shear flow turbulence (e.g. the experimental discovery and understanding of the mechanism of turbulent decay, generation, and evolution) present a variety of problems and a great challenge to one's abilities and technique. We decided to investigate the correlation of the wall pressure with the two velocity components parallel to the wall and stream and normal to the wall and stream. The interpretation of the measurements was guided by the theory for the wall pressure first developed by Kraichnan¹ and later extended and further developed by Lilley and Hodgson¹².

The only previous pressure-velocity correlation measurements reported in the literature are those of Kawamura¹³ and Serafini¹⁴. Kawamura measured the correlation between the wall pressure fluctuations and the longitudinal velocity fluctuations at zero time delay when the hot wire was directly above the pressure transducer. Kawamura's results do not agree with the present work for reasons which are not definitely known. The discrepancy may be caused by disturbances in the free stream (Kawamura reported a low signal-to-noise ratio), limitations of the pressure transducer or by disturbances from the trip. Serafini's results are in better qualitative agreement with our measurements than Kawamura's but in our opinion also show the effects of extraneous disturbances either outside the boundary layer or originating far upstream in the boundary layer.

The present investigation was carried out in a 5 inch thick turbulent boundary layer at a nominal free stream velocity of 206 ft/sec. The ratios of pressure transducer diameter and hot wire length to boundary layer thickness were approximately 1:30 and 1:100 respectively, allowing a study of the detailed structure of the fluctuations in the layer.

2. EXPERIMENTAL APPARATUS AND PROCEDURE

2.1 Wind Tunnel Facility

The experiments were carried out in the boundary layer on the floor of the 5 by 7 feet low speed wind tunnel facility at the Aeronautical Engineering Laboratories, The University of Michigan. More detailed information about the experimental equipment and environment can be found in our previous paper¹¹.

A schematic diagram showing the general lay-out is given in Figure 1. Natural transition took place in the contraction section and no tripping device was required

to make the boundary layer fully turbulent. A varnished and waxed sheet of masonite extending 14 feet upstream from the point of measurement was installed to make the wall aerodynamically smooth. In order to eliminate the undesirable effects of wind tunnel vibration, measurements were made on a 1 inch thick smooth (oil-lapped) steel plate, 20 inches in diameter and mounted on a heavy pedestal, which was inserted flush with the floor. The 1/16 inch gap which was allowed between the plate and the wind tunnel floor was sealed on the outside of the tunnel with a strip of rubber. The mounting pedestal was vibration-isolated from the floor by means of rubber shock pads. Holes were drilled in the plate to accept the pressure transducer assembly; holes not in use at any given time were filled with brass plugs which were fitted within ± 0.001 inch of the surface.

2.2 Instrumentation

The fluctuating wall pressure was measured with a pressure transducer¹⁵ made from two 0.163 inch diameter lead-zirconate disks mounted back to back in a brass body which was supported in the steel plate by rubber O-rings. A schematic diagram of the transducer installation is shown in Figure 2. The transducer was connected through a low-noise cable to a low-noise preamplifier having a cathode follower input with an input impedance of 1.2×10^8 ohms. The crystal capacity was 285 micro-microfarads, allowing a low frequency response down to approximately 5 cycles/sec. The gain of the preamplifier was approximately 50; it was followed by a two-stage amplifier which gave the entire system a maximum gain of 100,000. The bandwidth of the amplifier circuitry was adjustable between 1 cycle/sec and 160 kilocycles/sec.

The fluctuating velocities were measured with constant current hot wire equipment manufactured by Shapiro and Edwards. The frequency response of the uncompensated amplifier was flat from 0.13 cycle to 320 kilocycles. Adjustable filters in the amplifier were used to cut out frequencies above and below the range needed in the experiments to eliminate unnecessary noise. Tungsten wires 0.0002 inch in diameter and approximately 0.050 inch long were attached to the supports by the usual method of copper plating and soldering. The time constant of the wires was approximately 0.40 millisecond. The compensation required to correct for the time lag of the wires was determined by the square wave method and accomplished by a resistance-capacitance network in the amplifier. No wire length corrections were applied to any of the data because the microscale of the turbulence near the wall that was calculated from the measured spectra was found to be only twice the hot wire length. Moreover, the upper frequency limit on the tape recorder limits the smallest eddy which can be studied to a scale of approximately twice the hot wire length.

In the inner 0.2 of the boundary layer a micrometer screw was used to position the hot wire probe. The probe was located by measuring the distance between the hot wires and their surface reflection. At $y/\delta > 0.2$ the probe position was measured with an ordinary scale. A drawing of the hot wire probe for the closest spacing to the pressure transducer is also shown in Figure 2.

The signals from the pressure and velocity transducers were recorded on a three-channel Ampex Model FR-1100 magnetic tape recorder which utilized 1/2 inch wide tape traveling at 60 in./sec. This recorder has a bandwidth extending from d-c to 10 kilocycles which provided the limiting upper frequency for the measurements. A special

play-back unit was designed for the recorder with one movable head to allow the introduction of time delay between a pair of signals. The least increment in time delay was 0.017 millisecond.

The correlator used in the measurement of the space-time correlations worked on the mean-square principle. A thermocouple was used to measure the mean-square values of each of the two signals to be correlated, of their sum, and of their difference. The sum was obtained from a simple resistive summing circuit built into the apparatus, and the difference was obtained by first sending one signal through an electronic phase inverter and then into the summing circuit. A provision for external filtering of the sum and difference signals allowed the measurement of correlations in adjustable frequency bands; a Krohn-Hite Model 310-AB filter was used for this purpose. The output from the thermocouple was measured on a Sensitive Research d.c. millivoltmeter having a time constant of 3 seconds and the individual measurements were used to compute the correlation.

The spectral measurements were made using a fixed band-pass General Radio Model 736-A wave analyzer of the heterodyne type. The thermocouple circuitry in the correlator described above was used to obtain the mean-square value of the fluctuating output from the wave analyzer. Root-mean-square measurements were made with a Ballantine Model 320 true rms meter. Electrical signals were monitored with a DuMont Model 322-A dual-beam oscilloscope.

For the measurements of the correlation of pressure with velocity derivative, the velocity signal from the tape recorder was fed into a simple resistance-capacitance differentiating network having a linear response up to 10 kilocycles. The attenuated output was amplified and fed into the correlator.

3. EXPERIMENTAL ENVIRONMENT

3.1 Extraneous Disturbances

The accuracy of the measurements to be reported herein will be affected by the extraneous disturbances which are present. These include the vibration of the measuring apparatus, the sound field in the wind tunnel, the free stream turbulence level, and the mean flow conditions in the boundary layer. A comprehensive discussion of the sound measurements and flow visualization studies which were carried out is given in Reference 11. A short summary of the results will be given here.

A check on the effectiveness of the vibration isolation of the mounting showed that the spurious pressure signals caused by vibration amounted to less than 1/100 of the mean-square turbulent pressure fluctuations.

The sound field in the test section was first measured by a pressure transducer located on the stagnation line of an airfoil-shaped body exposed to the free stream. The spectrum of the stagnation pressure fluctuations had peaks at 135 and 200 cycles/sec. The wall pressure correlation measurements described in Reference 11 which were made later showed a small peak at negative time delay which was caused by sound propagating upstream. From these data it was finally determined that the mean-square sound pressure in the free stream amounted to approximately 1/20 of the mean-

square turbulent wall pressure fluctuations. The mean-square velocity fluctuations associated with the sound were less than 1/2 per cent of the mean-square turbulent fluctuations near the edge of the boundary layer.

The settling chamber of the wind tunnel contains four turbulence damping screens. The free-stream turbulence level in the test section increases with velocity and has been measured at 50, 100, and 150 ft/sec. Extrapolation of the data to the 200 ft/sec speed used in this experiment results in a value of $\frac{\sqrt{u^2}}{U_\infty} = 1 \times 10^{-3}$ for the turbulence level of the axial velocity component. The level of the transverse velocity component is approximately three times the level of the axial component.

Large-scale flow disturbances in the test section boundary layer were first discovered during the measurements of the wall pressure spectra which are described below. The entire wind tunnel, with the exception of the test section, is exposed to the weather. Heat transfer through the steel walls caused by sunlight impinging on the outside of the tunnel produced density stratification near the walls which in turn produced vorticity when accelerated into the test section. Observations of streamers of smoke near the concave surface of the contraction section showed large-scale oscillations which were swept into the test section. It is believed that the large-scale disturbances observed in the test section are caused by a combination of the Taylor-Goertler boundary layer instability on the concave walls of the contraction and the density stratification.

3.2 Properties of the Turbulent Boundary Layer used in the Investigation

All measurements were made with natural transition in the boundary layer which occurred approximately 24 feet ahead of the measuring points.

3.2.1 Mean Velocity Profiles

The mean velocity profiles were measured with a total head tube; the static pressure was measured on the wall. No correction was made for the effect of turbulence on the mean values. Since the data presented in this Report were taken over a period of time when the ambient temperature outdoors changed by some 20°, velocity profiles were taken at the extremes of temperature. The results were plotted in non-dimensional form in Figure 3. The wall friction velocity was obtained from a measurement of the wall shear stress with a Stanton tube using the calibration results reported by Gadd¹⁶. Also shown in Figure 3 is the ideal turbulent boundary layer profile of Coles¹⁷.

The properties of the measured boundary layer profile are tabulated in the following Table together with the properties of Coles' ideal boundary layer at the same value of R_θ , the Reynolds number based on momentum thickness. Figure 3 and the Table below show that there is satisfactory agreement with the ideal case.

**Comparison of Boundary Layer Parameters with
Coles' Ideal Turbulent Boundary Layer Parameters**

T^0 (F.)	U_∞	R_θ	δ	δ^*	θ	δ^*/θ	U_τ/U_∞	R	Remarks
67	204	38,000	0.42	0.041	0.0315	1.30	0.0326	3.1×10^7	Present investigation.
		38,000					1.30	3.2×10^7	Coles' ideal boundary layer based on same R_θ .
45	203	43,000	0.42	0.041	0.0315	1.30	0.0325	3.85×10^7	Present investigation.
		43,000					1.295	4.0×10^7	Coles' ideal boundary layer based on same R_θ .

3.2.2 Wall Pressure Spectrum[†]

The non-dimensional spectrum of the wall pressure is shown in Figure 4. The data were always repeatable for $\frac{\omega\delta^*}{U_\infty} > 0.13$, but were not repeatable for $\frac{\omega\delta^*}{U_\infty} < 0.13$

($f < 105$ cycles/sec). The spectral density below $\frac{\omega\delta^*}{U_\infty} = 0.13$ varied with the amount of heat transfer to the tunnel by sunlight. This variation is believed to be caused by the large-scale disturbances which arise from the density stratification discussed earlier in Section 3.1.

In the measurements of mean-square pressure and velocity and space-time correlation of pressure with velocity the Krohn-Hite filter has been used to reject all frequencies below $\frac{\omega\delta^*}{U_\infty} = 0.13$. The upper limit on the frequency, $\frac{\omega\delta^*}{U_\infty} = 12.5$, was provided by the tape recorder response.

It is shown by the pressure-velocity correlation measurements reported in Section 4 that the disturbances at any height in the boundary layer are convected at the local mean speed. At the closest spacing of the hot wire to the wall, 0.050 inch, the local speed is approximately $0.58 U_\infty$. Since the boundary layer thickness is 0.42 foot, disturbances convected at this speed which produce pressure fluctuations at $\frac{\omega\delta^*}{U_\infty} = 0.13$ have a wave-length of 2.7δ . Hence, even with filtering information can be obtained about eddies whose scale is at least $2\frac{1}{2}$ times the boundary layer thickness.

[†] Recently we have measured the spectra with four different size transducers. The results are shown in Figure 42 and discussed in the Appendix.

The root-mean-square wall pressure was 2.64 times the wall shear stress[†] and 5.61×10^{-3} times the free stream dynamic pressure.

3.2.3 Velocity Intensity Profiles

The intensity profiles of the velocity fluctuations measured in the frequency band $0.13 < \frac{\omega \delta^*}{U_\infty} < 12.5$ are shown in Figure 5. A comparison with the work of Klebanoff⁵ shows that in the present case there are higher intensity levels in the inner half of the boundary layer and lower levels in the outer half of the layer for all three turbulence components. However, there are two main differences in the experimental conditions. In the present investigation, the boundary layer was produced by natural transition, whereas Klebanoff used sandpaper roughness on the leading edge of his plate to trip the boundary layer. Also, the Reynolds number based on momentum thickness in the present experiment is approximately six times as large as Klebanoff's value. It should be noted that Klebanoff and Diehl¹⁸ measured the u intensity profile in 1952 under the same operating conditions as those of Klebanoff⁵ in 1955 and found values as much as 30 per cent higher. Accordingly, it is believed that the intensity profiles of the turbulence in the boundary layer which are measured in any given case will be affected by the properties of the tripping device, if any, which is used and will depend upon the value of the Reynolds number in some unknown way. This idea is supported by the measurements of Reference 11 which showed that either wall roughness or a boundary layer trip acted to increase the root-mean-square wall pressure.

The intensity profile of the longitudinal derivative of the velocity component normal to the wall, $\frac{\partial v}{\partial x}$, is shown for the inner half of the boundary layer in

Figure 6. A comparison with the data of Klebanoff⁵ shows that the present results are approximately $2\frac{1}{2}$ times as large near the wall and $1\frac{1}{2}$ times as large near the center of the layer. It is believed that this discrepancy is also caused by either the boundary layer trip used by Klebanoff or the difference in Reynolds number.

3.2.4 Velocity Spectra

The power spectra of the u and v velocity fluctuations which were measured directly with the wave analyzer have been converted to wave number spectra by assuming that the disturbance at any height is convected at the local mean speed and decays slowly. In this case the wave number is defined by

$$k = \frac{\omega}{U} \quad (1)$$

and the relation

$$E(k) = UE(\omega) \quad (2)$$

[†] This value is different from that quoted in our earlier paper¹¹. An error was made in the computation of $\sqrt{(p^2)}$. Recent measurements of $\sqrt{(p^2)}$ with four different size transducers are discussed in the Appendix.

holds. The spectra which are shown in Figures 7 and 8 are normalized to have unit area above $\frac{\omega \delta^*}{U_\infty} = 0.13$. The values of the spectral density corresponding to $\frac{\omega \delta^*}{U_\infty} = 0.13$ are marked by the flagged point on each curve.

The non-dimensional u spectra, $\frac{UE_u(\omega)}{U}$, scale with the local non-dimensional wave number, $k\delta^* = \frac{\omega \delta^*}{U}$, except for the spectrum at the closest spacing to the wall at large wave number. This result implies that the disturbances in the frequency band under consideration are convected at the local mean speed. Moreover, the disturbances must be decaying slowly with time in this frequency band since only in the case of a completely frozen flow with no decay would the u spectra collapse perfectly into one universal curve. The spectrum near the wall at large wave number deviates from the other spectra because the small scale disturbances which are relatively abundant near the wall decay or are deformed (elongated) relatively rapidly.

These data can be compared with the velocity-velocity correlation data obtained by others. The wave number spectral density, $E_u(k)$, is the transform of the longitudinal spatial correlation of the u velocity component; i.e.,

$$E_u(k) = 2 \frac{\overline{u^2}}{\pi} \int_0^\infty R_{uu}(x_1) \cos kx_1 dx_1. \quad (3)$$

If $E_u(k)$ is a function of k only, as the present data show, then $R_{uu}(x_1)$ must be a universal function which is independent of the height in the boundary layer. Hinze¹⁹ reports that the shape of the correlation curves $R_{uu}(x_1)$ measured by many investigators (see, e.g., Grant⁶) is independent of height except near $x_1 = 0$. The shape of $R_{uu}(x_1)$ near $x_1 = 0$ is governed by the behavior of the spectrum at large wave number (see Hinze¹⁹) and the non-uniform behavior of R_{uu} in this region is believed to be caused by the decay of the large wave number (small scale) fluctuations. For the same reason the spectral curves of $E_u(k)$ must separate at high wave number. The upper frequency in the present investigation was limited by the tape recorder response, and the data do not extend to a high enough wave number to show this effect. However, the separation at high wave number is shown by the data obtained by Klebanoff⁵ who obtained measurements at frequencies higher than those studied in the present investigation.

In the outer half of the boundary layer, Klebanoff's u spectra in the frequency band corresponding to the present measurements also scaled with the wave number based on the local velocity. In the inner half of the layer, however, the spectral curves were separated. The normalized curves showed relatively more high frequency energy near the wall. It is not known at this time whether this disagreement with the present data is an effect of the different Reynolds number or of the trip which was used by Klebanoff. However, the shape of the curve obtained from the present non-dimensionalized spectral measurements agrees well with the shape of the curve obtained by Klebanoff.

The normalized v spectra shown in Figure 8 do not scale with the wave number based on local velocity. Equivalent behavior is found by other investigators (see, e.g., Grant⁸) who have measured the longitudinal correlation of the v velocity and found the shape of $R_{vv}(x_1)$ to depend upon the height in the layer[†]. Therefore, it cannot be determined from the spectral curves whether or not the v disturbance is also convected at the local speed. However, the measurements of correlation between pressure and velocity which are presented in Section 4 establish that this is the case.

The v spectra at the two points farthest from the wall exhibit humps near $\frac{\omega \delta^*}{U} = 0.4$. It is believed that these anomalies in the v spectra are caused by the large-scale extraneous disturbances discussed in Section 3.1

4. EXPERIMENTAL MEASUREMENTS

The first measurements of the correlation of the wall pressure with the velocity components were made with the hot wires placed directly above the pressure transducer as shown in Figure 2. We first investigated the magnitude of the spurious pressure fluctuations produced by the unsteady flow field and wake of the hot wire probe. Measurements of the root-mean-square wall pressure and spectrum were made with the hot wire probe as close to the wall as possible, $\frac{x_2}{\delta^*} = 0.10$. The root-mean-square pressure and power spectrum of the pressure were not changed if the hot wires were downstream or directly above the transducer. The spectrum at all frequencies and the root-mean-square pressure were increased whenever the hot wires were upstream of the pressure transducer ($x_1 < 0$). For this reason, we have not reported any measurements with the hot wires upstream of the pressure transducer.

The electrical signals from the hot wires and pressure transducer were filtered before the correlation was measured. Signals outside the frequency band $105 < f < 10,000$ cycles/sec were rejected because we have found, Reference 11 and Section 3.1, that there are large scale low frequency disturbances in the flow outside the boundary layer. The upper limit, 10,000 cycles/sec, of the filter band is determined by the limit of the electronic system of the tape recorder.

4.1 Measurements of the Correlations \overline{pu} and \overline{pv}

The pressure-velocity correlation coefficients that have been measured are defined by

[†] These results imply that the v velocity fluctuation near the wall decays at a faster rate than the u velocity fluctuation in this region. This finding agrees with the results of the pressure-velocity correlation measurements described in Section 4 which show that near the wall the R_{pv} correlation decays faster than the R_{pu} correlation.

$$R_{pu}(x_1, x_2, x_3; \tau) = \frac{\overline{p(x, 0, z; t) u(x+x_1, x_2, z+x_3; t+\tau)}}{\sqrt{\overline{p^2(x, 0, z; t) u^2(x+x_1, x_2, z+x_3; t)}}}, \quad (4)$$

$$R_{pv}(x_1, x_2, x_3; \tau) = \frac{\overline{p(x, 0, z; t) v(x+x_1, x_2, z+x_3; t+\tau)}}{\sqrt{\overline{p^2(x, 0, z; t) v^2(x+x_1, x_2, z+x_3; t)}}}. \quad (5)$$

The experimental measurements are shown in Figures 9 through 26 as functions of the non-dimensional time delay $\frac{U_\infty(\tau-\tau')}{\delta^*}$. The shift of the origin on the time delay axis, given by $\frac{U_\infty\tau'}{\delta^*}$, is computed at each value of $\frac{x_2}{\delta^*}$ by dividing the longitudinal spacing $\frac{x_1}{\delta^*}$ by the non-dimensional local mean speed $\frac{U}{U_\infty}$ at the hot wires. A vertical line on each curve shows the true origin, $\frac{U_\infty\tau}{\delta^*} = 0$.

At any given distance from the wall the correlation coefficients, R_{pu} and R_{pv} , that were measured with the hot wires in the plane parallel to the stream and normal to the wall that contains the pressure transducer (the $x_3 = 0$ plane) have nearly the same shape when plotted as a function of $\frac{U_\infty(\tau-\tau')}{\delta^*}$. (See Figs. 9 to 26.) This means that the pressure-velocity correlation is produced by the convected eddies in the boundary layer which move at the local mean speed. The effect of the decay or deformation of the eddies as they are carried along by the stream can be observed from these correlation measurements if the shape of the correlation curves, as a function of τ , measured at small $\frac{x_1}{\delta^*}$ is compared with the shape of the correlation curve measured at the same distance from the wall but with larger $\frac{x_1}{\delta^*}$. This comparison shows that the extreme values of the correlation are slightly reduced in magnitude and the spacing in time delay, τ , is slightly increased. The effect of the decay and distortion is greatest when the hot wires are near the wall.

When the rate of change of the shape of the correlation curves is small (for small values of $\frac{x_1}{\delta^*}$) it is possible to infer the approximate correlation that would be measured at an upstream position of the hot wires, by assuming that there is no change in shape of the correlation curve as a function of τ , measured at downstream positions, and then interchanging any given time delay with the spatial separation distance computed by assuming that the eddies are convected at the local speed. The relation between x_1 and τ that was used for the interchange of spatial separation and time delay is

$$\frac{x_1}{\delta^*} = - \frac{(\tau - \tau') U_\infty}{\delta^*} \frac{U(y)}{U_\infty} \quad (6)$$

The error introduced by this assumption for small spatial or temporal separations has been checked. We have made two correlation measurements with the hot wires upstream of the transducer ($\frac{x_1}{\delta^*} = -0.51$, $\frac{x_2}{\delta^*} = 0.51$, $x_3 = 0$ and $\frac{x_1}{\delta^*} = -1.02$, $\frac{x_2}{\delta^*} = 1.02$, $x_3 = 0$) and found that the maximum errors near the extreme values of R_{pv} and R_{pu} were ± 20 per cent and ± 10 per cent respectively. When the spatial separation or time delay is large, the effect of evolution or decay of the eddies is important but we have not attempted to estimate the error in this case because the wake of the hot wire probe could not be avoided with our method of hot wire mounting.

The correlation coefficients R_{pu} and R_{pv} were also measured at points downstream of the pressure transducer and in planes $x_3 = \text{const.}$ which do not contain the pressure transducer. The correlations measured for $x_3 > 0$ are also shown in Figures 9 to 26.

Using these measurements and converting time delay to spatial separation we have constructed contours of constant correlation in the three orthogonal planes, $x_1 = \text{const.}$, $x_2 = \text{const.}$, and $x_3 = 0$. The results are displayed in Figures 32 to 37. The most remarkable feature of these correlation contours is that almost everywhere the values of R_{pu} and R_{pv} have opposite signs. We have been able to qualitatively explain this behavior in Section 5. We also note for future reference in Section 5 that the correlation contours in the x_1, x_3 plane change character as one approaches the wall.

The measurements of R_{pu} and R_{pv} can be mapped in the $x_3 = 0$ plane in a form that we have called the 'vector field of the correlations'. The field is constructed with the origin at the pressure transducer and with

- (i) the length of the vector at any point equal to $\sqrt{(R_{pu}^2 + R_{pv}^2)}$, where the correlations are based on the local root-mean-square values of the velocity fluctuations, and
- (ii) the direction of each vector, measured from the positive x_1 -axis, is given by $\tan^{-1} \frac{R_{pv}}{R_{pu}}$ where the wall pressure pulse is assumed to be negative.

The assumption that the pressure is negative when R_{pu} and R_{pv} have opposite signs causes the rotation of the vector field in Figure 41 to be clockwise, which is reasonable from a consideration of the mean shear. From this orderly behavior of R_{pu} and R_{pv} it is proposed that the vortex filaments in the turbulent eddies with axis primarily in the x_3 direction make the major contribution to the wall pressure fluctuations.

4.2 Measurements of the Correlation $\overline{pv_x}$

The correlation of the wall pressure with $\frac{\partial v}{\partial x}$ is of interest from the point of

view of Kraichnan's¹ original formulation of the wall pressure problem in which only the first order linear term that produces the wall pressure is considered. Early in the course of our investigation, G.M. Corcos suggested that we plan to measure $\overline{pv_x}$ because this correlation is likely to give us the most direct information about the linear source term for the wall pressure. Section 5 contains a discussion of this theory and relates it to these experiments.

The quantity $\frac{\partial v}{\partial x}$ is difficult to measure with hot wires especially near the wall.

We have used the fact that the turbulence is convected at approximately the local speed in the boundary layer to again determine a spatial variation in the stream direction, x_1 , of a property of the turbulence from the time variation of the property measured by a stationary observer. We used the transformation

$$\frac{\partial v}{\partial x} = -\frac{1}{U_c} \frac{\partial v}{\partial t} \quad (7)$$

In this way the relation between the correlation coefficients

$$R_{pv_x} = \frac{\overline{p(x, 0, z; t) v_x(x+x_1, x_2, z+x_3; t+\tau)}}{\sqrt{\overline{p^2}(x, 0, z; t) \overline{v_x^2}(x+x_1, x_2, x_3; t)}} \quad (8)$$

and

$$R_{p\dot{v}} = \frac{\overline{p(x, 0, z; t) \dot{v}(x+x_1, x_2, z+x_3; t+\tau)}}{\sqrt{\overline{p^2}(x, 0, z, t) \overline{\dot{v}^2}(x+x_1, x_2, z+x_3; t)}} \quad (9)$$

is

$$R_{pv_x} = -R_{p\dot{v}} \quad (10)$$

where $\dot{v} = \frac{\partial v}{\partial t}$. The relation between the previously measured correlation coefficient R_{pv} and $R_{p\dot{v}}$ is

$$R_{p\dot{v}} = \sqrt{\left(\frac{v^2}{\dot{v}^2}\right)} \frac{\partial}{\partial \tau} (R_{pv}) \quad (11)$$

From the experimental point of view, it is easier to measure $R_{p\dot{v}}$ directly by differentiating the v velocity signal electrically and then measuring the correlation with the pressure than it is to use the relation of Equation 11.

The values of the correlation coefficient, $R_{p\dot{v}}$ measured directly by electrical differentiation, Figures 29 through 31, were again plotted versus the non-dimensional time delay $\frac{U_\infty(\tau-\tau')}{\delta^*}$. A vertical line on each curve for $\frac{x_1}{\delta^*} = 0$ shows the true origin

$\frac{\tau U_\infty}{\delta^*} = 0$. These measurements again illustrate the fact that the convection speed of the velocity disturbance which is correlated with the wall pressure is equal to the local mean speed.

The measurements of $R_{p\dot{v}}$ as a function of τ were used in the same way as before, see Section 4.1 and Equation (6), to construct the contours of constant correlation coefficient $R_{p\dot{v}}$ in the planes $x_1 = 0$, $x_2 = \text{const.}$ and $x_3 = 0$ that are shown in Figures 38 through 40. These correlation contours are probably as accurate as those of R_{pu} and R_{pv} because the same data and methods of plotting were used. However, the quantity $R_{p\dot{v}}$ is supposed to represent $-R_{pvx}$; but there is an additional error when we interpret $-R_{p\dot{v}}$ as R_{pvx} because we have determined a spatial variation twice from the idea of a convected slowly changing eddy, once to determine $\frac{\partial v}{\partial x}$ and again to infer the upstream values of R_{pvx} . We have not measured or estimated our errors but they are certainly larger than the ± 20 per cent maximum error in R_{pv} discussed in Section 4.1.

4.3 Influence of External Disturbances on the Pressure-Velocity Correlations

The total effect of disturbances in the flow and the errors in our measurements may be assessed by comparing our measurements with the integral condition of Phillips²⁰. The condition is that the surface integral of the spatial correlation of the wall pressure with any dynamical quantity in the turbulence must vanish over any plane parallel to the wall. We are indebted to Professor G.M. Lilley for bringing this condition to our attention. We have checked to see if the conditions

$$\iint_{-\infty}^{\infty} R_{pu} dx_1 dx_3, \quad \iint_{-\infty}^{\infty} R_{pv} dx_1 dx_3, \quad \iint_{-\infty}^{\infty} R_{p\dot{v}} dx_1 dx_3 = 0 \quad (12)$$

are satisfied in the three planes with $\frac{x_2}{\delta^*}$ equal to 0.10, 0.20 and 0.51 of Figures 34, 37 and 40. We found that only the condition

$$\iint_{-\infty}^{\infty} R_{p\dot{v}} dx_1 dx_3 = 0 \quad (13)$$

was approximately satisfied only in the plane closest to the wall $\frac{x_2}{\delta^*} = 0.10$. In the eight other cases the surface integrals were large and negative. Some idea of the relative magnitude of the surface integral may be obtained from the fact that the negative values satisfied the inequality

$$0.4 < \frac{-\int_{-\infty}^{\infty} R dx_1 dx_3}{\int_{-\infty}^{\infty} |R| dx_1 dx_3} < 0.6 . \quad (14)$$

These computations were carried out by snipping out contours of constant correlation from uniform sheets of tracing paper and weighing them. There was great difficulty in deciding what the contour was for small correlation because the data of Figures 34, 37 and 40 are not complete at large distances. It does seem clear that there are still appreciable free stream disturbances which cause errors in the correlation measurements because the condition that the surface integrals, Equation (12), vanish is that the flow be homogeneous in the planes $x_2 = \text{const.}$ and that the spatial correlations between any two velocity components vanish with the inverse cube of the spatial separation between them anywhere in the flow.

The fact that the surface integral of R_{pv} over the plane nearest the wall is almost zero gives us some confidence that these measurements can be trusted for qualitative assessments of the nature of the relation between the wall pressure and the turbulence but use of these measurements for detailed quantitative conclusions is not justified until the reason that Phillips' ²⁰ integral condition was not satisfied is explained and taken into account.

The information about the flow disturbances that we have is worth considering. We have already mentioned, Section 3.1, that there were disturbances in the free stream outside the boundary layer. We know that there are low frequency sound waves in the test section moving upstream¹¹ which produce 5 per cent of the mean-square wall pressure. The wall pressure produced by the plane sound field will be negatively correlated with the u component of the velocity measured by the hot wire because the wave length of the sound (3 ft) is much greater than the spatial separation of the hot wire and wall pressure transducer. We have made a rough estimate of the change in the correlation R_{pu} caused by the sound field and find that the condition of a vanishing surface integral of R_{pu} is almost satisfied by accounting for the contribution from the sound field. For the integral over R_{pu} at $\frac{x_2}{\delta^*} = 0.51$ we corrected the value of the integral and found

$$-\int_{-\infty}^{\infty} R_{pu} dx_1 dx_3 / \int_{-\infty}^{\infty} |R_{pu}| dx_1 dx_3 \simeq 0.2 . \quad (15)$$

Thus the sound field is affecting the R_{pu} measurements. The contribution to R_{pu} from the sound was a small positive constant equal to $R_{pu} = 0.017$.

The correlations involving the velocity component normal to the wall will not be affected to first order by a plane sound wave propagating parallel to the wall and we can only conclude that other effects in the free stream disturb the correlation measurements.

A serious source of disturbances that can affect the R_{pv} and $R_{p\dot{v}}$ measurements are the density stratified flow and Taylor-Goertler vortices that exist in the tunnel¹¹. They can cause inhomogeneous turbulence in the x_3 direction affecting the v and w velocities and can also prevent the velocity correlations vanishing like the inverse cube of the separation distance.

We have made a few measurements to check the symmetry of the correlations R_{pu} and R_{pw} but unfortunately not R_{pv} , which is of more interest. One would expect the boundary layer to be homogeneous in the x_3 direction. R_{pu} and R_{pv} should be symmetric about $x_3 = 0$.

Symmetry of R_{pu} about $x_3 = 0$ was found in the measurements; see, for example, Figure 27. The correlation coefficient R_{pw} , defined in a similar manner to R_{pu} and R_{pv} , was measured at various values of $\frac{x_2}{\delta^*}$ in the two frequency bands $0.13 < \frac{\omega \delta^*}{U_\infty} < 12.5$ (the usual band) and $0.38 < \frac{\omega \delta^*}{U_\infty} < 12.5$. Some typical results are shown in Figure 28.

The measured correlation is small but definitely not zero, and has approximately the same scale throughout the boundary layer. The transverse scale across the stream is only about 0.1 of the longitudinal scale along the stream. Filtering out the frequencies below 300 cycles/sec $\left(\frac{\omega \delta^*}{U_\infty} = 0.38\right)$ destroys most of the correlation. The reason for the lack of symmetry of R_{pw} about $\frac{U_\infty \tau}{\delta^*} = 0$ is not known.

We are forced to conclude that the R_{pv} and $R_{p\dot{v}}$ correlations cannot be corrected because we do not have enough information about the disturbances in the tunnel. We believe that the measurements are qualitatively correct because the disturbances are undoubtedly small. Only a small error is required to prevent satisfaction of the integral condition. Another source of disturbances is the wall roughness. We have found¹¹ that wall roughness affects the pressure at all frequencies, not just at low frequencies. See the Appendix for an example of the effect of wall roughness.

5. QUALITATIVE COMPARISON OF KRAICHNAN'S WALL PRESSURE THEORY WITH THE EXPERIMENTAL RESULTS

It is useful to examine the existing approximate theory for the wall pressure fluctuations to see if our measurements seem reasonable in the light of the theory and to see what our measurements can tell us about the structure of turbulence. The basic idea for knowledge of the turbulence structure is that the pressure is a kind of weighted average, scalar property of the turbulent velocity field and one has the idea that an eddy can be followed by knowledge of the pressure field. Certain correlations of pressure and velocity may then reveal something about the nature of the turbulence.

3.1 A Brief Outline of the Theory for the Wall Pressure

The frame-work for these considerations is the theory first put forward by Kraichnan¹ and enlarged by Lilley and Hodgson¹². The results from the paper of Lilley and Hodgson¹² (which is very clear and easy to follow) will be used in the following summary of the theory.

Consider an incompressible viscous flow. The equations of motion are

$$\frac{\partial u'_j}{\partial x_j} = 0 \quad (16)$$

$$\rho \left(\frac{\partial u'_i}{\partial t} + u'_j \frac{\partial u'_i}{\partial x_j} \right) = - \frac{\partial p'}{\partial x_i} + \mu \frac{\partial^2 u'_i}{\partial x_j^2} . \quad (17)$$

An equation for the pressure is obtained from the divergence of the momentum equation

$$\frac{\partial^2 p'}{\partial x_j^2} = - \rho \frac{\partial^2 u'_i u'_j}{\partial x_i \partial x_j} . \quad (18)$$

To obtain an equation for the fluctuating pressure we substitute

$$p' = \bar{p} + p, \quad u'_i = \bar{u}_i + u_i \quad (19)$$

in Equation (18) and subtract the mean value of the equation. The result is

$$\frac{\partial^2 p}{\partial x_j^2} = - \rho \frac{\partial^2}{\partial x_i \partial x_j} (u_i u_j + u_i \bar{u}_j + u_j \bar{u}_i - \bar{u}_i \bar{u}_j) = -Q . \quad (20)$$

Lilley and Hodgson¹² show that a useful integral representation for the wall pressure is

$$p(\bar{x}, t) = \frac{1}{2\pi} \int_V Q(\bar{r}, t) \frac{dV(\bar{r})}{|\bar{r} - \bar{x}|} + 2 \int_S \frac{\partial}{\partial r_2} p(\bar{r}, t) \frac{dS(\bar{r})}{|\bar{r} - \bar{x}|} . \quad (21)$$

If the assumption that $\bar{u}_2 = \bar{u}_3 = 0$, $\bar{u}_1 = \bar{u}_1(x_2)$ and $\frac{u_i}{\bar{u}_1} \ll 1$ is made, the two largest (linear) terms in Q (the right hand side of Equation (20)) combine to give a 'source' term representing the interaction of turbulence with the mean shear

$$Q \approx 2\rho \frac{\partial \bar{u}_1}{\partial x_2} \frac{\partial u_2}{\partial x_1} . \quad (22)$$

The use of only these linear terms for Q was originally justified by Kraichnan¹ who showed that, approximately, the sum total of all other terms, caused by turbulence-turbulence interaction, contribute a root-mean-square value of the pressure that is 10 db lower than the contribution from the two linear terms. It is this approximation

that needs experimental verification and is discussed below. The next step consists in showing from available experiments near the wall that the surface integral of Equation (21) makes a negligible contribution to the wall pressure in comparison with the volume integral over the turbulence-mean shear term of Equation (22) (see Lilley and Hodgson¹² for a clear explanation).

On this basis, the mean-square wall pressure receives a major contribution from the interaction of the turbulence with the mean shear. The integral representation for the wall pressure, Equations (21) and (22), then becomes

$$p(o,t) = \frac{\rho}{\pi} \int_V \frac{\partial \bar{u}_1(r_2)}{\partial r_2} \frac{\partial u_2(\vec{r}, t)}{\partial r_1} \frac{dV(\vec{r})}{|\vec{r}|} \quad (23)$$

where the origin of the coordinate system is the point on the wall where the pressure is computed. The pressure velocity correlations are

$$\overline{p(o,t) u_1(\vec{x}, t + \tau)} = \frac{\rho}{\pi} \int_V \frac{\partial \bar{u}_1(r_2)}{\partial r_2} \frac{\partial}{\partial r_1} \left[\overline{u_2(\vec{r}, t) u_1(\vec{x}, t + \tau)} \right] \frac{dV(\vec{r})}{|\vec{r}|} \quad (24)$$

$$\overline{p(o,t) u_2(\vec{x}, t + \tau)} = \frac{\rho}{\pi} \int_V \frac{\partial \bar{u}_1(r_2)}{\partial r_2} \frac{\partial}{\partial r_1} \left[\overline{u_2(\vec{r}, t) u_2(\vec{x}, t + \tau)} \right] \frac{dV(\vec{r})}{|\vec{r}|} \quad (25)$$

A qualitative comparison of our measurements of R_{pu} and R_{pv} with these expressions can be made if we integrate Equations (24) and (25) with respect to r , by parts.

We assume the correlations of $\overline{u_2 u_1}$ and $\overline{u_2 u_2}$ vanish sufficiently rapidly as functions of $|\vec{r} - \vec{x}|$ to insure the vanishing of the surface integrals. The result of the partial integration is

$$\overline{p(o,t) u_1(\vec{x}, t + \tau)} = \frac{\rho}{\pi} \int_V \frac{\partial \bar{u}_1(r_2)}{\partial r_2} \overline{u_2 u_1(\vec{r} - \vec{x}, \tau)} \frac{r_1}{|\vec{r}|} dV(\vec{r}) \quad (26)$$

$$\overline{p(o,t) u_2(\vec{x}, t + \tau)} = \frac{\rho}{\pi} \int_V \frac{\partial \bar{u}_1(r_2)}{\partial r_2} \overline{u_2 u_2(\vec{r} - \vec{x}, \tau)} \frac{r_1}{|\vec{r}|} dV(\vec{r}) \quad (27)$$

We will not normalize the correlations in our further discussion which involves only the signs and zeros of the correlations.

5.2 Qualitative Comparison of the Wall Pressure Produced by Interaction of the Turbulence and Mean Shear

Comparisons between the above expressions, Equations (26) and (27), and the experiments will be made first for the R_{pv} correlation. Grant⁸ has reported numerous measurements of the \overline{vw} correlation in his studies of the large eddies in the boundary layer. He found that at distances from the wall greater than $\frac{y}{\delta} = 0.29$, \overline{vw} was essentially positive for any orientation of the separation distance, $|\vec{r} - \vec{x}|$, between the measuring points. For our purpose this means that the contribution of \overline{vw} to the integral representation for \overline{pv} , Equation (27), will be essentially positive for $\frac{y}{\delta} > 0.3$. The sign of the correlation \overline{pv} will then be determined by the location, x , of the hot wire that measures the v velocity. The sign of \overline{pv} at zero time delay should be positive when the hot wire is downstream, $x_1 > 0$, of the pressure transducer because there $r_1 > 0$ and the integrand is essentially positive. In the same way \overline{pv} should be negative when $x_1 < 0$, and approximately zero when the hot wire is in the plane $x_1 = 0$ containing the pressure transducer. If we consider the contours of constant correlation of R_{pv} of Figures 35, 36 and 37, we see that for $\frac{y}{\delta} \geq 0.51$ the above considerations are approximately satisfied.

We may also consider the correlation $\overline{pv_x}$ on the same basis. The formula for $\overline{pv_x}$ may be written

$$\overline{p(0,t) \frac{\partial u_2(\vec{x}, t + \tau)}{\partial x_1}} = -\frac{\rho}{\pi} \int_V \frac{\partial \overline{u_1}(r_2)}{\partial r_2} \frac{\partial^2}{\partial r_1^2} [\overline{u_2 u_2}(\vec{r} - \vec{x}, \tau)] \frac{dV(\vec{r})}{|\vec{r}|} \quad (28)$$

where we have used the fact that $\overline{u_2(\vec{r})u_2(\vec{x})}$ is a function of $(\vec{r} - \vec{x})$ so that

$$\overline{u_2(\vec{r}, t) \frac{\partial u_2(\vec{x}, t + \tau)}{\partial x_1}} = -\frac{\partial}{\partial r_1} \overline{u_2 u_2}(\vec{r} - \vec{x}, \tau). \quad (29)$$

Integrating Equation (28) by parts twice over r_1 , and again assuming that the \overline{vw} correlations decay rapidly enough to insure the vanishing of the surface integrals, one obtains

$$\overline{p(0,t) \frac{\partial u_2(\vec{x}, t + \tau)}{\partial x_1}} = \frac{\rho}{\pi} \int_V \frac{\partial \overline{u_1}(r_2)}{\partial r_2} \overline{u_2 u_2}(\vec{r} - \vec{x}, \tau) \frac{r_2^2 + r_3^2 - 2r_1^2}{|\vec{r}|^5} dV(\vec{r}). \quad (30)$$

With the same argument given before, based on the positive contribution of \overline{vw} , it is apparent that $\overline{pv_x}$ should vanish on the surface of two half cones with their axes in the wall extending upstream and downstream and centered on the pressure transducer. The cone half angle is $\tan^{-1} \sqrt{2}$. Outside the half cones $|r_2|, |r_3| > \sqrt{2}|r_1|$ the correlation $\overline{pv_x}$ should be positive and \overline{pv} negative; see Equations (30) and (10).

Inside the half cones $|r_2|$, $|r_3| < |(2)r_1|$ the signs of $\overline{pv_x}$ and \overline{pv} change. If we consider the contours of constant \overline{pv} of Figures 38, 39 and 40, we see that for $\frac{x_2}{\delta^*} \geq 0.51$ these considerations are approximately satisfied.

There is not much information available about the spatial dependence of the \overline{uv} correlation that controls the behavior of the \overline{pu} correlation in Equation (26). We know that the shear stress at a point is negative and the correlation coefficient $-\frac{\overline{uv}}{\sqrt{(u^2v^2)}}$ has a value of approximately one-half. If we assume that \overline{uv} is essentially negative for any orientation of the distance separating the measuring points we find, in the same manner as for \overline{pv} , that \overline{pu} should have the opposite value of \overline{pv} everywhere and should also be zero on the plane $x_1 = 0$. These conditions are also approximately satisfied for $0.5 < \frac{x_2}{\delta^*} < 6.0$.

5.3 Qualitative Discussion of the Turbulence Structure Near the Wall

The most interesting feature of pressure velocity correlations is their behavior very near the wall. Let us consider \overline{pv} . Near the wall in the planes $\frac{x_2}{\delta^*} = 0.20$ and 0.10 the constant correlation contours of \overline{pv} show a curious swept-back behavior (see Fig. 37). The value of \overline{pv} is positive for some regions where $x_1 < 0$. Consider the lines $x_1 = \pm x_3$ for $x_1 < 0$; it is apparent that the integral of Equation (27) must be receiving negative contributions in these regions from the \overline{vv} correlation. Grant⁸ did not report any measurements of \overline{vv} for $\frac{x_2}{\delta^*} < 0.29$. We have made a few measurements of \overline{vv} very near the wall that will be reported in a later paper when they are more complete. We have found that \overline{vv} has appreciable negative values along a line $x_3 = \pm x_1$ for $x_1 < 0$ in agreement with the idea that negative \overline{vv} can cause the behavior of \overline{pv} that we observe.

The point of interest here is the structure of the turbulent eddies very near the wall where the turbulence is generated. It appears to us that there is a definite structure that is worth understanding. Our measurements can probably be explained on the basis that there are hairpin-shaped vortices very near the wall that cause the change in the \overline{pv} and \overline{pu} correlation contours near the wall. Work on this problem is continuing.

5.4 Discussion of the Effect of Turbulence-Turbulence Interaction Terms on the Wall Pressure

Using our tape recorded data for p , u and v , we have tried to measure the pressure velocity squared correlations $\overline{pu^2}$ and $\overline{pv^2}$ that are representative of two of the triple correlation source terms representing turbulence-turbulence interaction

with mean shear that enter into the expression for the mean-square wall pressure. There are also quadruple velocity correlations that should be considered in a discussion of this nature. We have not tried to measure these terms.

The $\overline{pu^2}$ and $\overline{pv^2}$ measurements gave very small R_{pu^2} and R_{pv^2} correlation coefficients. The largest values were of the order of 0.04 and it is to be noted that the accuracy of these small values is very much in doubt. The measured values are certainly very small. The question of direct experimental verification that the sum total of the many turbulence-turbulence interaction terms contributes 10 db less to the root-mean-square wall pressure than the turbulence-mean shear interaction term may not be answered until better techniques and cleaner flows are developed. One can make the argument that if $\overline{pu^2}$ and $\overline{pv^2}$ are small, and they are, then none of the other higher order terms can possibly be large in the random turbulence field.

Our measurements definitely show that the gross spatial properties of pressure-velocity correlations exhibit the behavior one would expect if the wall pressure were produced by turbulence-mean shear interaction. Thus, turbulence-mean shear interaction does produce a large portion of the wall pressure.

6. CONCLUSIONS

The main results of this experimental investigation can be summarized as follows:

- (i) Evidence has been accumulated that a boundary layer trip has a rather severe effect on the properties of turbulence in the boundary layer. From a study of the data of other investigators and a comparison with the present investigation, it is evident that a trip acts to increase the wall pressure intensity and the velocity intensity near the wall. The experiments of Grant² and Favre^{3,4} show that the integral scale of the longitudinal velocity correlation is also affected by the trip used. It now appears that some features of the turbulent structure obtained in many of the previous investigations in tripped boundary layers were not always universal but were a function of the experimental conditions imposed by the tripping device.
- (ii) The convection speed of the velocity disturbance at any point which is correlated with the wall pressure disturbance is the local mean speed at that point.
- (iii) The measurements of the \overline{pv} correlations display the correct features that one would expect on the basis that a large fraction of the wall pressure is produced by the interaction of turbulence with the mean shear.
- (iv) The measurements of \overline{pv} and \overline{pu} are subject to disturbances from the free stream that prevent the satisfaction of Phillips'²⁰ integral condition on the correlation of the wall pressure with a dynamical turbulence property. Quantitative calculations of the wall pressure based on these pressure-velocity correlation data may be in error for this reason. Even though the error in \overline{pv} and \overline{pu} is small (10 per cent), quantitative calculations

involve integrals over large regions, thus allowing a large error to be made. See Section 4.3.

- (v) The measurements of the R_{pv} correlation show that the convection speed of the wall pressure disturbance should not exceed $0.9 U_\infty$, the local speed at $y/\delta \approx 0.4$, because R_{pv} is very small above this height. The measured¹¹ convection speed was $0.83 U_\infty$ at large transducer spacing and the restriction is satisfied. The speed $0.83 U_\infty$ occurs in the boundary layer profile at $y/\delta = 0.22$.
- (vi) The measurements of R_{pv} and $R_{p\dot{v}}$ very near the wall show a definite structure that one would expect from hairpin-shaped vortices in the region of turbulent production. The \overline{vv} correlations also change character in a region very near the wall.

7. ACKNOWLEDGMENTS

We wish to thank Professors A.M. Kuethé, M.S. Uberoi and E.G. Gilbert for helpful discussions and suggestions. The assistance of Messrs. B.J. Tu and F. Roos is appreciated. This work has been supported by the Mechanics Branch Office of Naval Research, Contract Nonr-1224(30).

REFERENCES

1. Kraichnan, R.H. *Pressure Fluctuations in Turbulent Flow over a Flat Plate.* J. Acoust. Soc. Amer., 28, 1956, p. 378.
2. Townsend, A.A. *The Structure of the Turbulent Boundary Layer.* Proc. Camb. Phil. Soc., 47, 1951, p. 375.
3. Schubauer, F.B.
Klebanoff, P.S. *Investigation of the Separation of the Turbulent Boundary Layer.* NACA Rep. No. 1030, 1951.
4. Laufer, J. *The Structure of Turbulence in Fully Developed Pipe Flow.* NACA Rep. No. 1174, 1955.
5. Klebanoff, P.S. *Characteristics of Turbulence in a Boundary Layer with Zero Pressure Gradient.* NACA Tech. Note No. 3178, 1954.
6. Corsin, S.
Kistler, A.L. *The Free-Stream Boundaries of Turbulent Flows.* NACA Tech. Note. No. 3133, 1954.
7. Favre, A.J.
et alii *Space-Time Double Correlations and Spectra in a Turbulent Boundary Layer.* J. Fluid Mech., 2, 1957, p. 313; J. Fluid Mech., 3, 1958, p. 344.
8. Grant, H.L. *The Large Eddies of Turbulent Motion.* J. Fluid Mech., 4, 1958, p. 149.
9. Bull, M.K. *Properties of the Fluctuating Wall-Pressure Field of a Turbulent Boundary Layer.* Univ. of Southampton, A.A.S.U., Rep. 234, 1963.
10. Corcos, G.M. *Pressure Fluctuations in Shear Flows.* Univ. of Calif. Inst. of Eng. Research Report Ser. 183, No. 2, 1962.
11. Willmarth, W.W.
Wooldridge, E.E. *Measurements of the Fluctuating Pressure at the Wall Beneath a Thick Turbulent Boundary Layer.* J. Fluid Mech., 14, 1962, p. 187.
12. Lilley, G.M.
Hodgson, T.H. *On Surface Pressure Fluctuations in Turbulent Boundary Layers.* AGARD, Rep. 276, 1960.
13. Kawamura, M. *Pressure-Velocity Correlation and Double Velocity Correlation in a Turbulent Boundary Layer Along a Flat Plate.* J. Sci. Hiroshima Univ., Ser. A, 24, 1960, p. 403.
14. Serafini, J.S. *Wall Pressure Fluctuations in a Turbulent Boundary Layer.* Case Institute of Tech., Ph.D. Thesis, 1962.

15. Willmarth, W.W. *Small Barium-Titanate Transducer for Aerodynamic or Acoustic Pressure Measurements.* Rev. Sci. Inst., 29, 1958, p. 218.
16. Gadd, G.E. *A Note on the Theory of the Stanton Tube.* Brit. R. and M. 3147, 1960.
17. Coles, D. *Measurements in the Boundary Layer on a Smooth Flat Plate In Supersonic Flow. I. The Problem of the Turbulent Boundary Layer.* Jet Prop. Lab. Rep. 20-69, 1953; or A.A.M.P., V, 1954, p. 181.
18. Klebanoff, P.S.
Diehl, Z.W. *Some Features of Artificially Thickened Fully Developed Turbulent Boundary Layers with Zero Pressure Gradient.* NACA Rep. 1110, 1952.
19. Hinze, J.O. *Turbulence.* New York: McGraw-Hill Book Company, 1959, Chapter 1.
20. Phillips, O.M. *On the Aerodynamic Surface Sound from a Plane Turbulent Boundary Layer.* Proc. Roy. Soc. (London), A, 234, 1956, p. 327.
21. Uberoi, M.S.
Kovaszny, L.S.G. *On Mapping and Measurement of Random Fields.* Quarterly Applied Math., X, 1953, p. 375.
22. Willmarth, W.W. *Statistical Properties of the Pressure Field in a Turbulent Boundary Layer.* WADC Tech. Rep. 59-676, 1961, p. 109.
23. Corcos, G.M. *Resolution of Pressure in Turbulence.* J. Acous. Soc. Am., 35, 1963, p. 192.

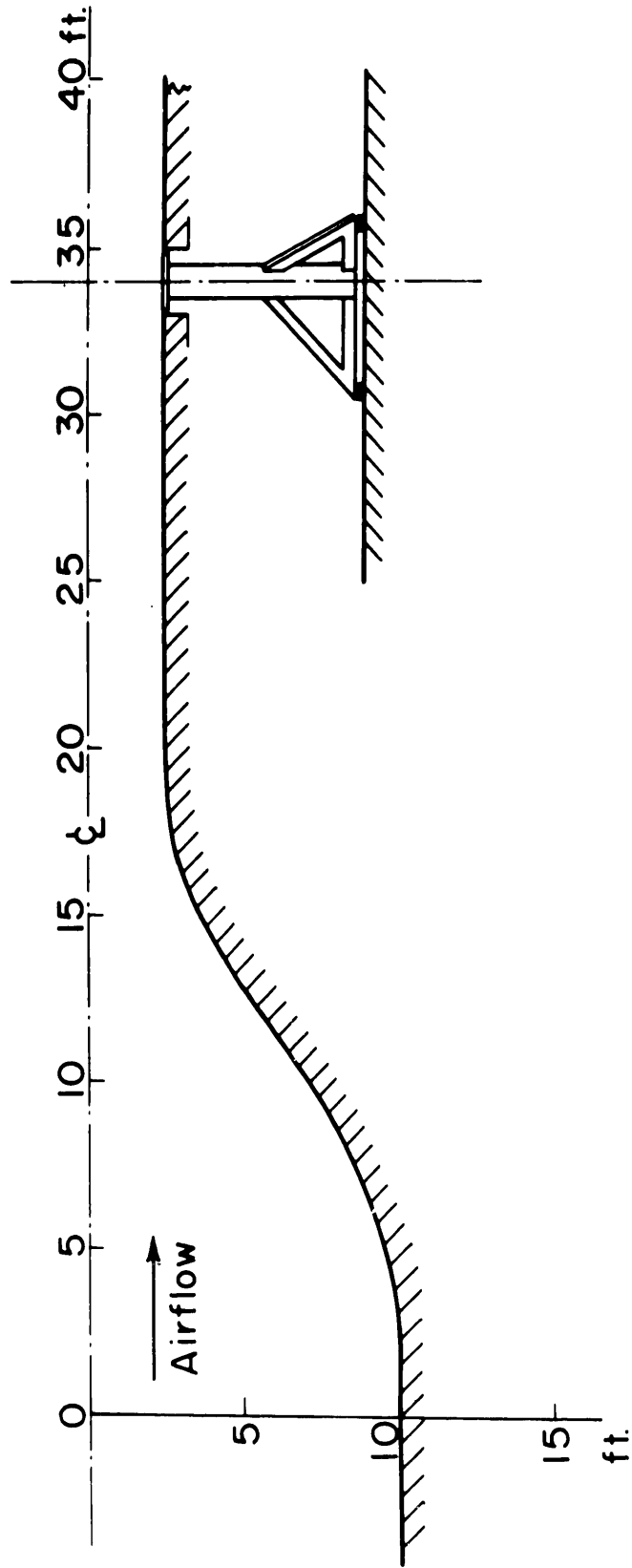


Fig.1 Scale drawing of wind tunnel test section and massive vibration isolation mounting for the transducers

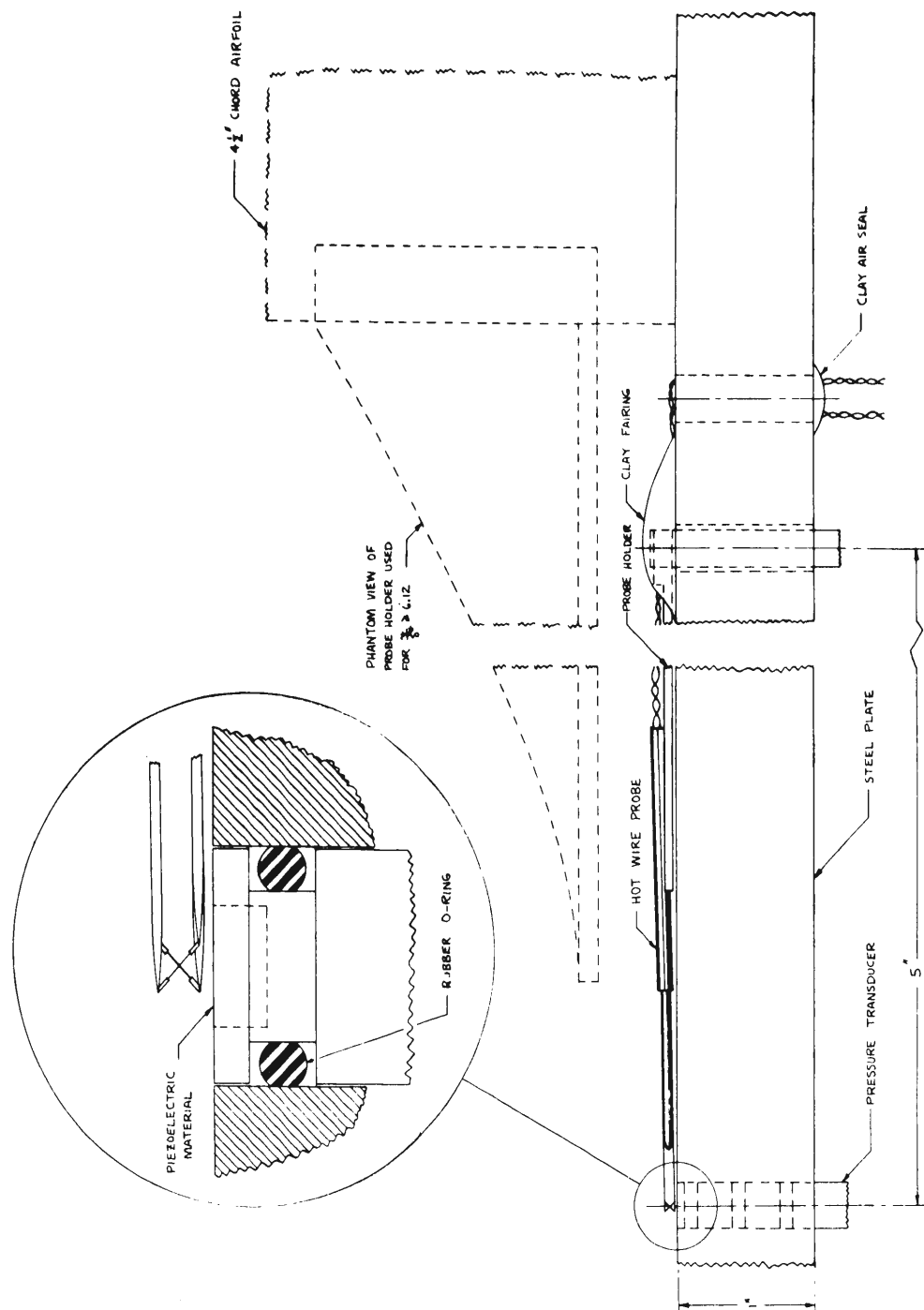


Fig. 2 Pressure transducer and hot wire installation. Hot wire shown at closest spacing to plate, 0.050 inch

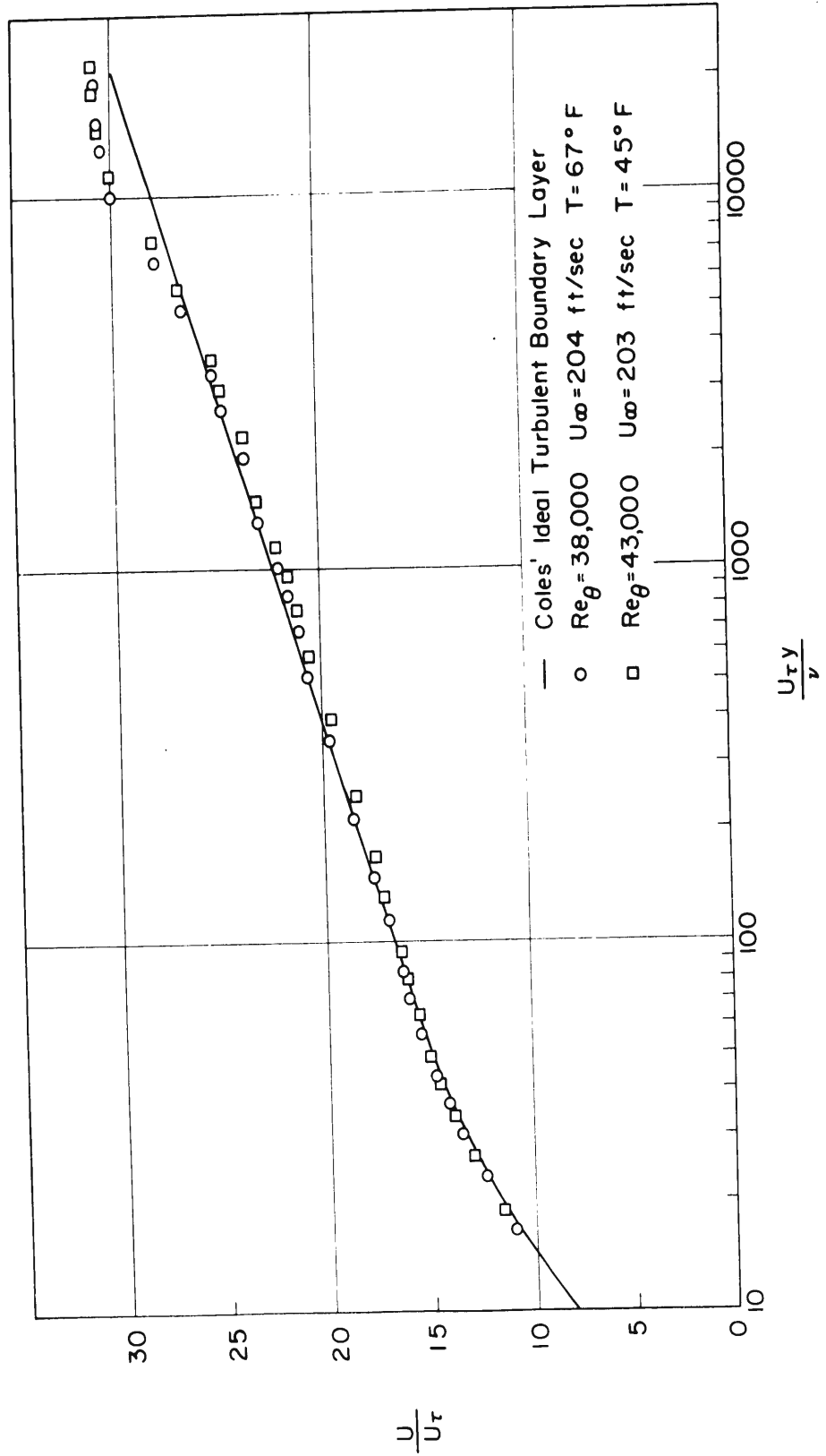


Fig. 3 Mean velocity profiles in the turbulent boundary layer. Refer to Table on page 6 for other boundary layer parameters

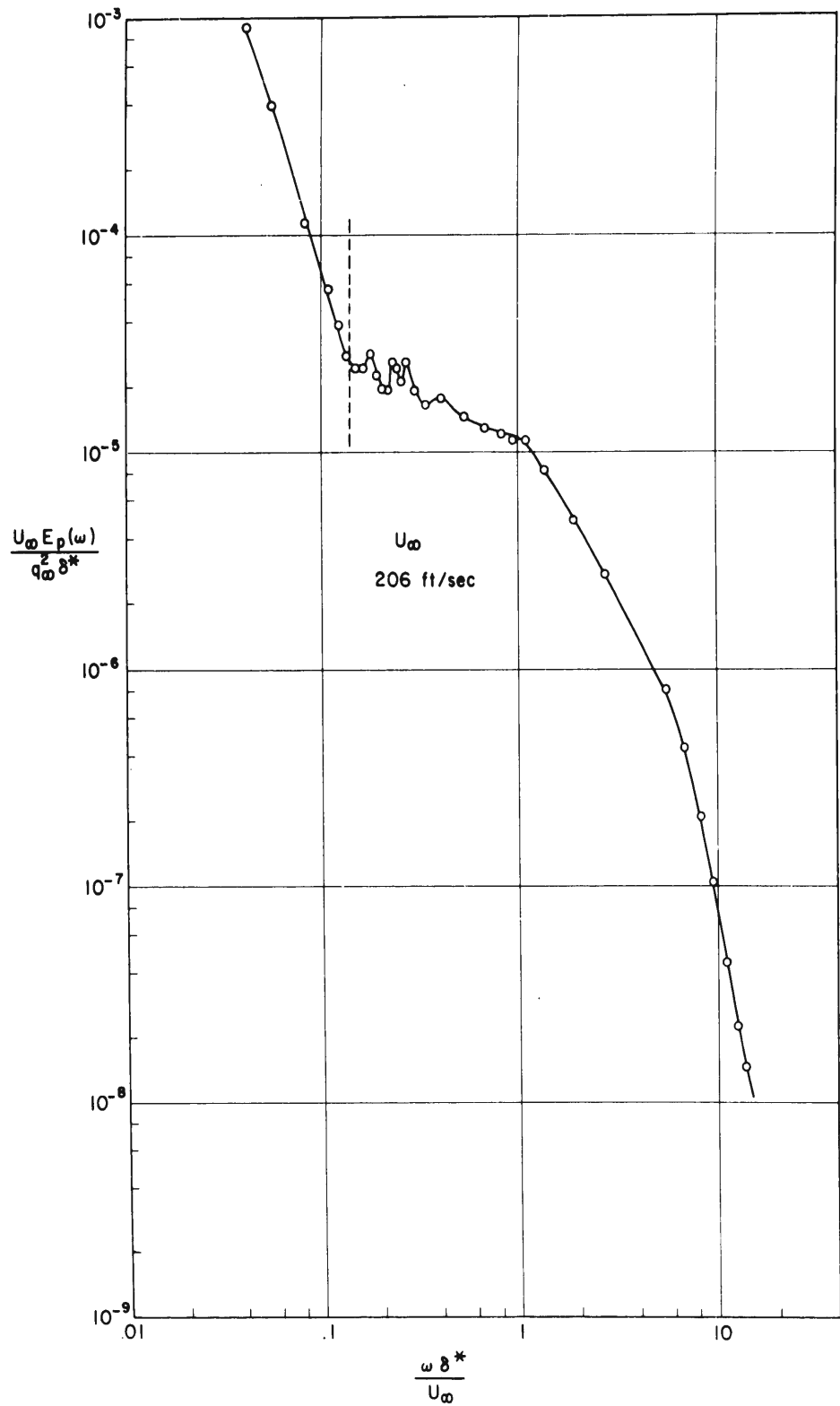


Fig.4 Dimensionless power spectrum of the wall pressure. Vertical dashed line shows the frequency below which signals were rejected in the subsequent measurements

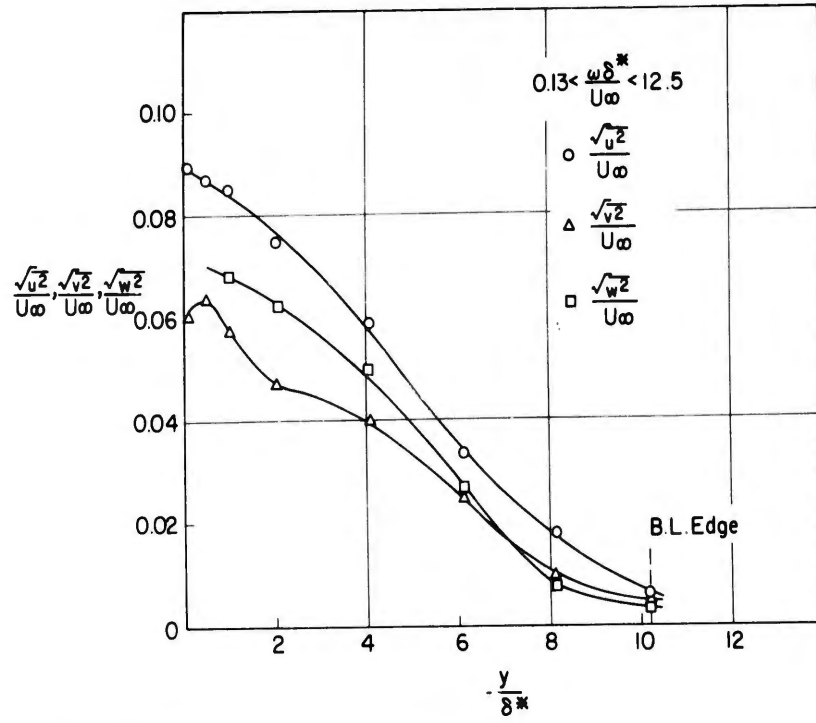


Fig.5 Turbulent velocity intensity profiles in the frequency band used in the subsequent experiments

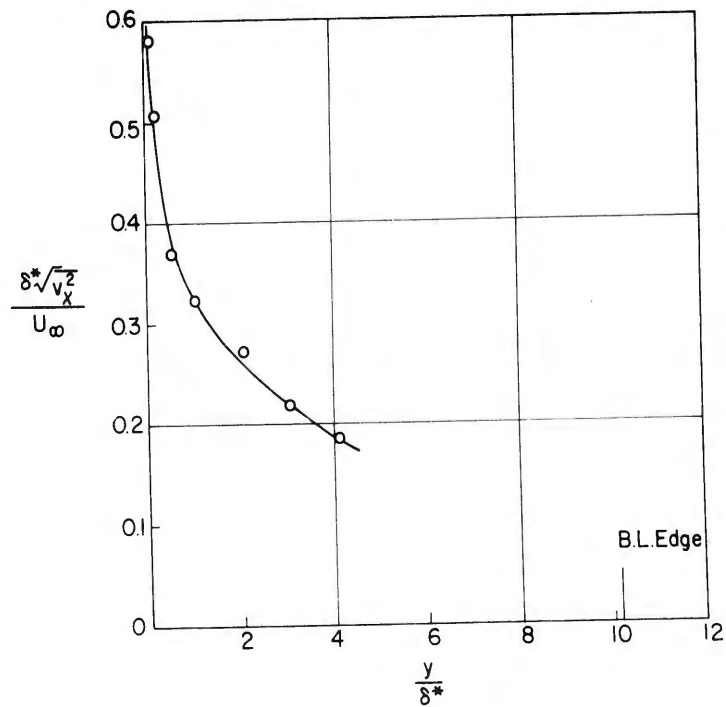


Fig.6 Intensity profile of longitudinal derivative of velocity normal to wall

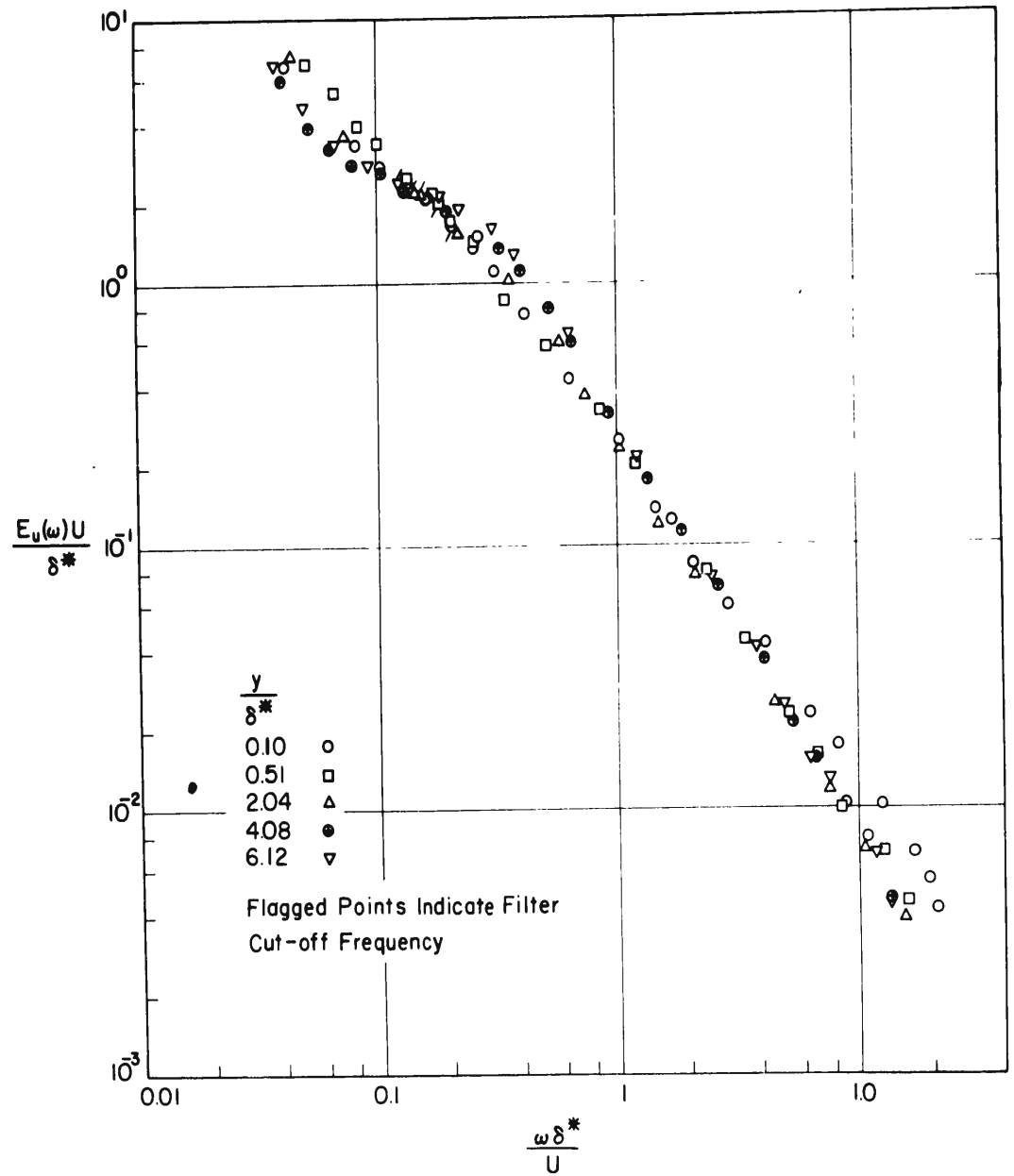


Fig.7 Dimensionless normalized power spectra of the longitudinal velocity components at various heights in the boundary layer. Spectra are normalized to have unit area in the frequency band of the subsequent experiments

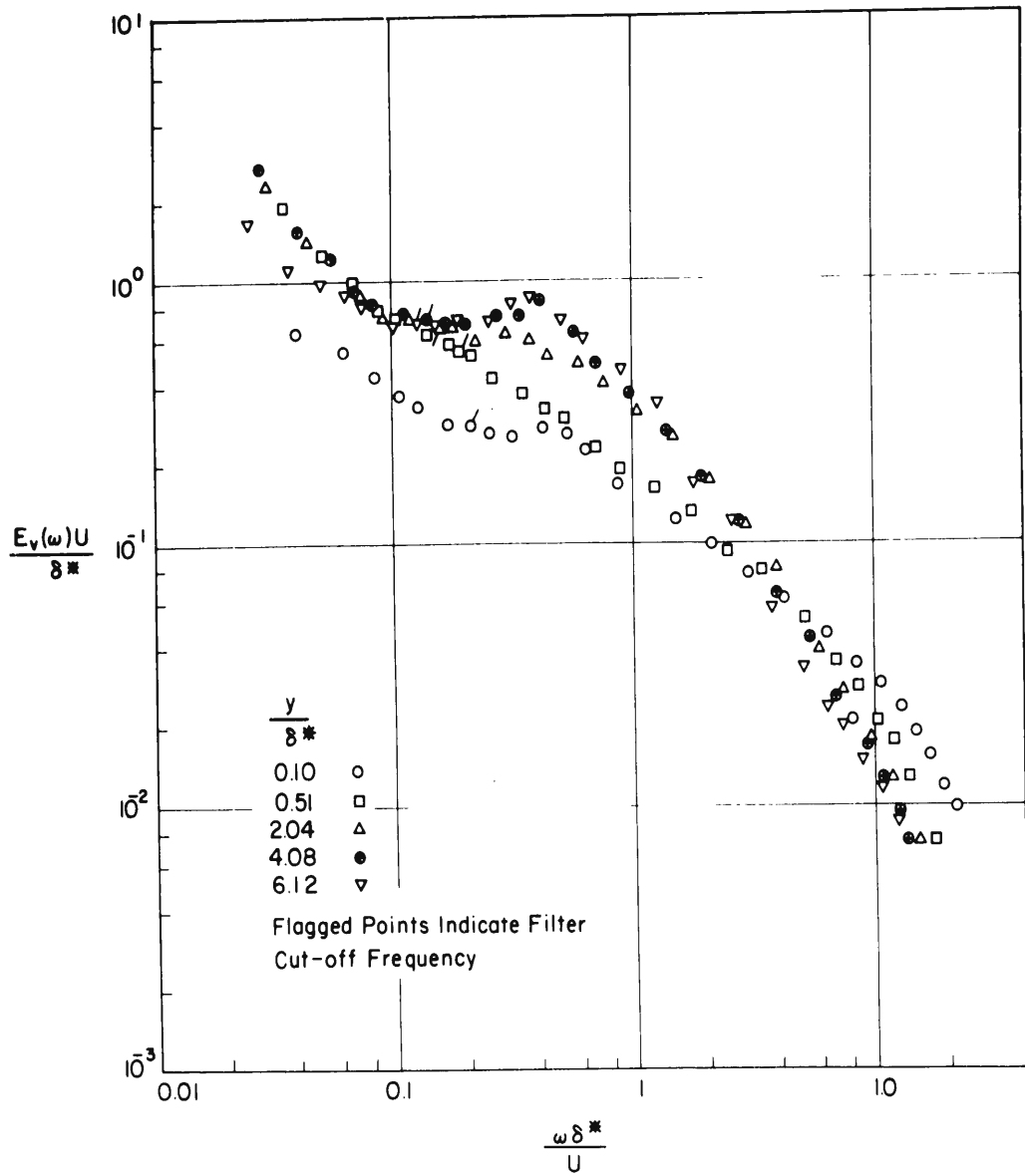


Fig. 8 Dimensionless normalized power spectra of the velocity components normal to the wall at various heights in the boundary layer. Spectra are normalized to have unit area in the frequency band of the subsequent experiments

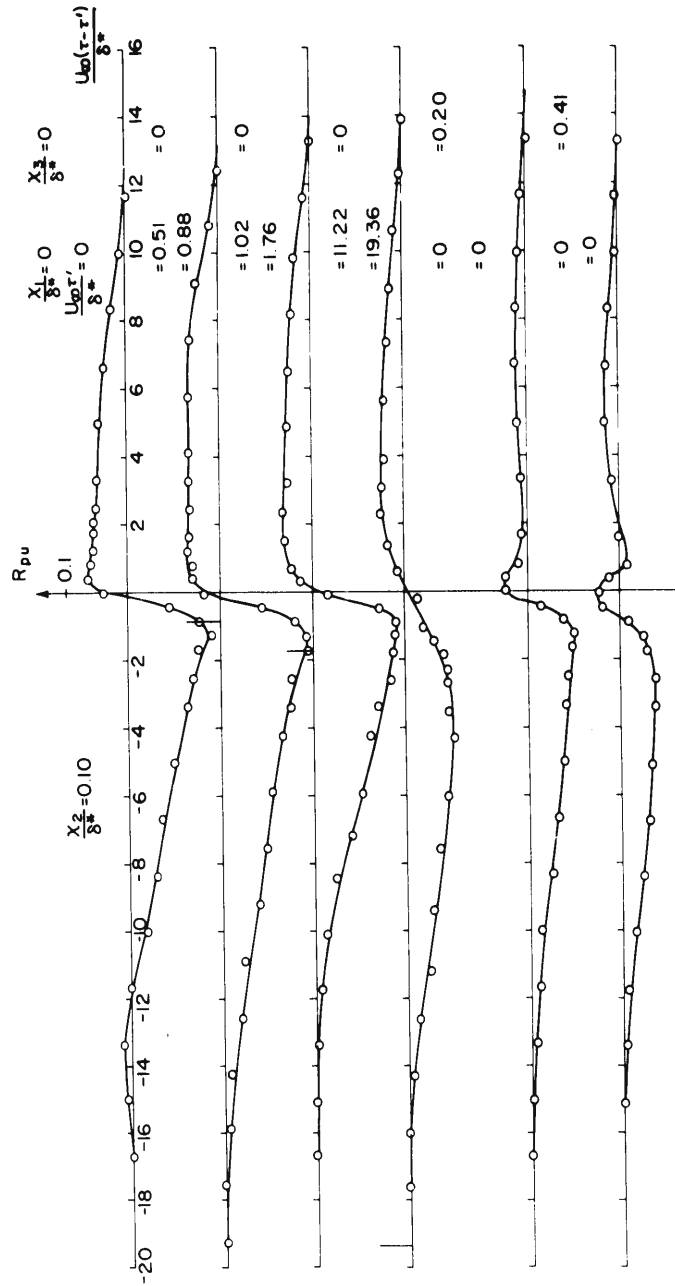


Fig. 9 Measured values of the space-time correlation of fluctuating velocity with fluctuating wall pressure

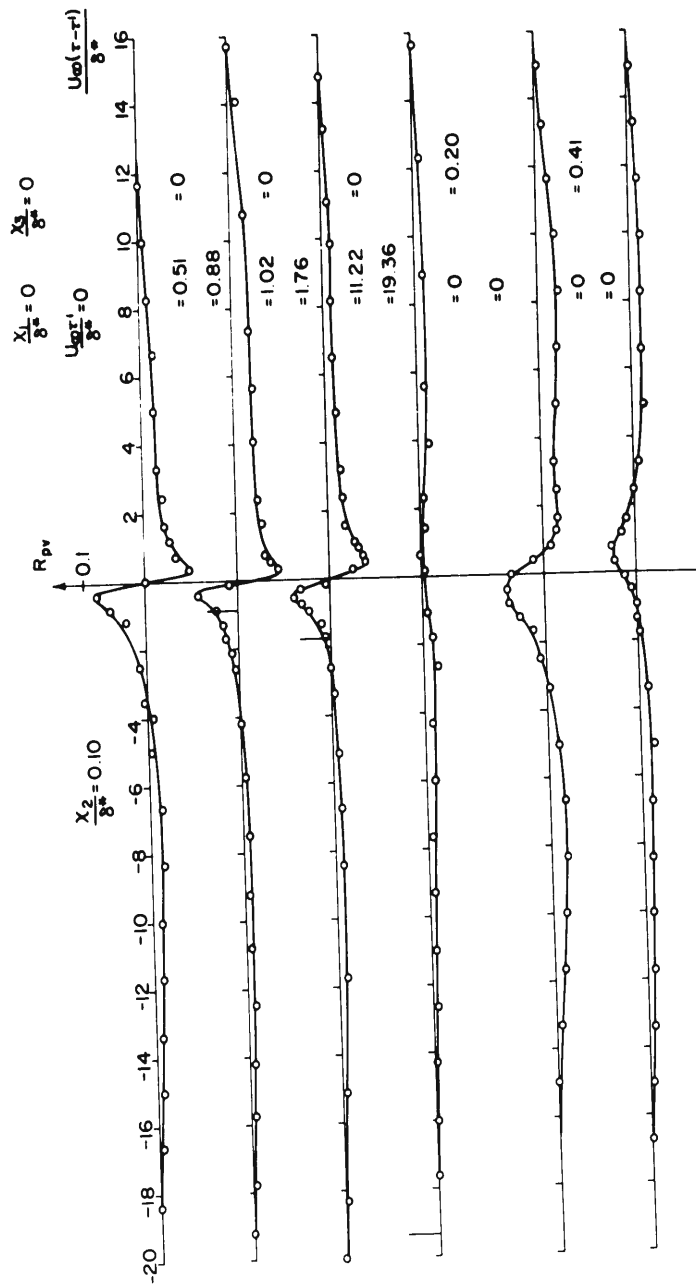


Fig. 10 Measured values of the space-time correlation of fluctuating velocity with fluctuating wall pressure

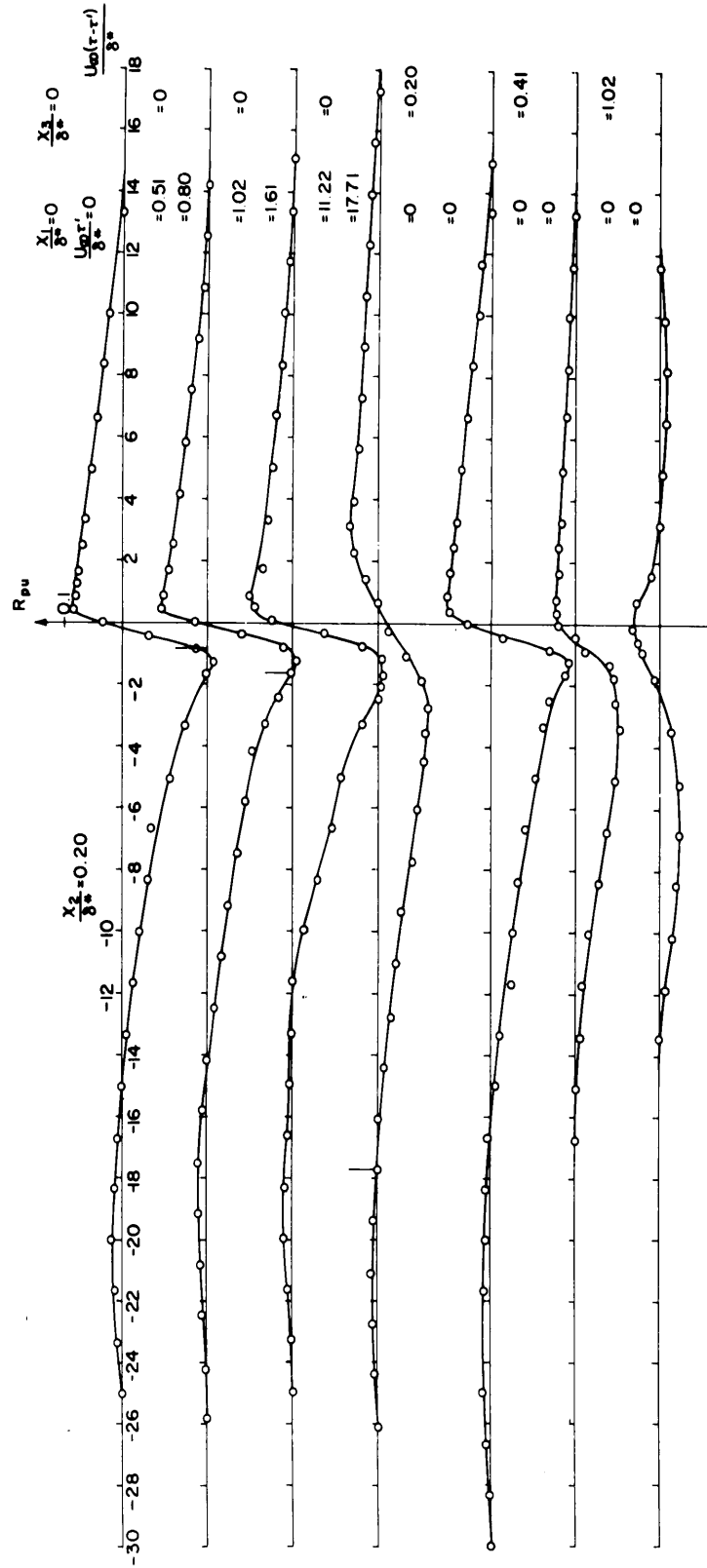


Fig. 11 Measured values of the space-time correlation of fluctuating velocity with fluctuating wall pressure

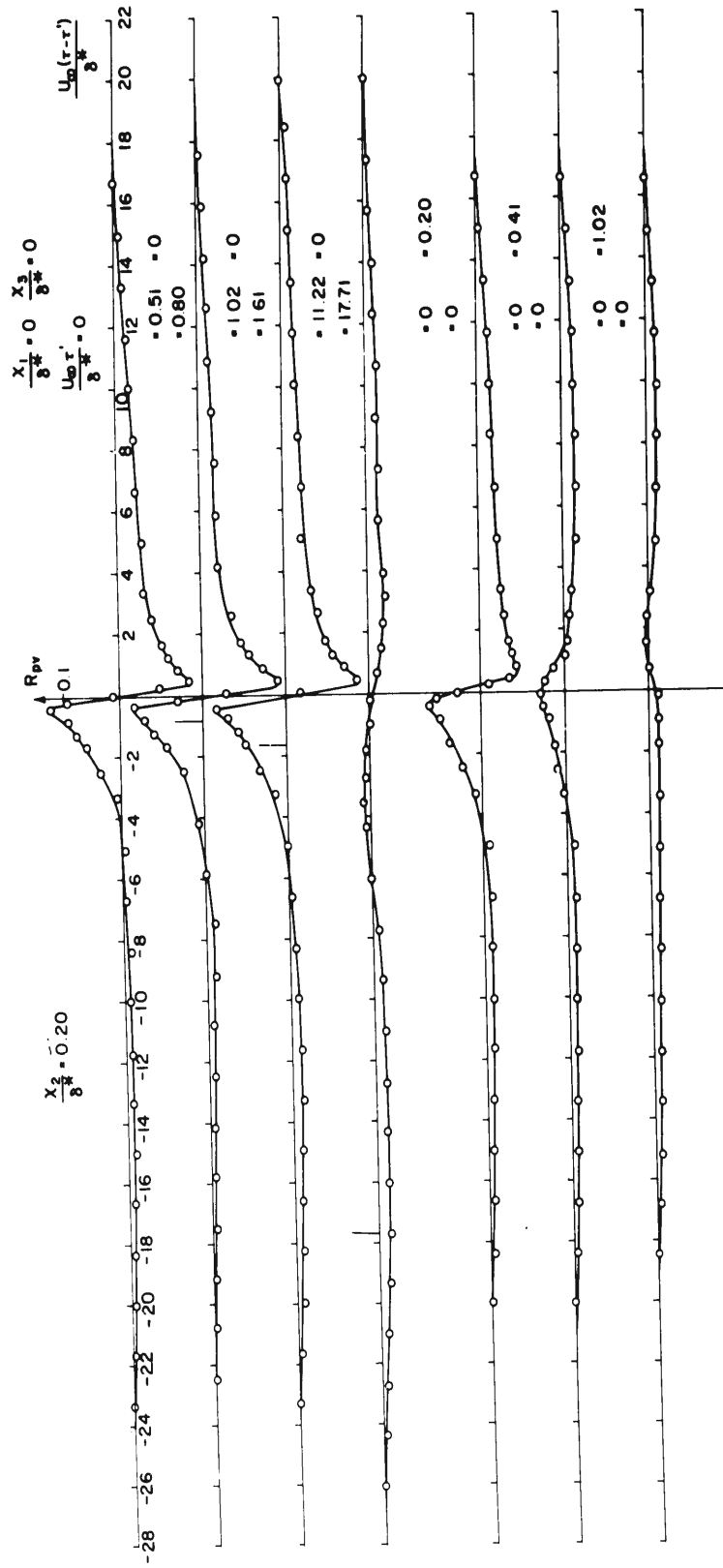


Fig. 12 Measured values of the space-time correlation of fluctuating velocity with fluctuating wall pressure

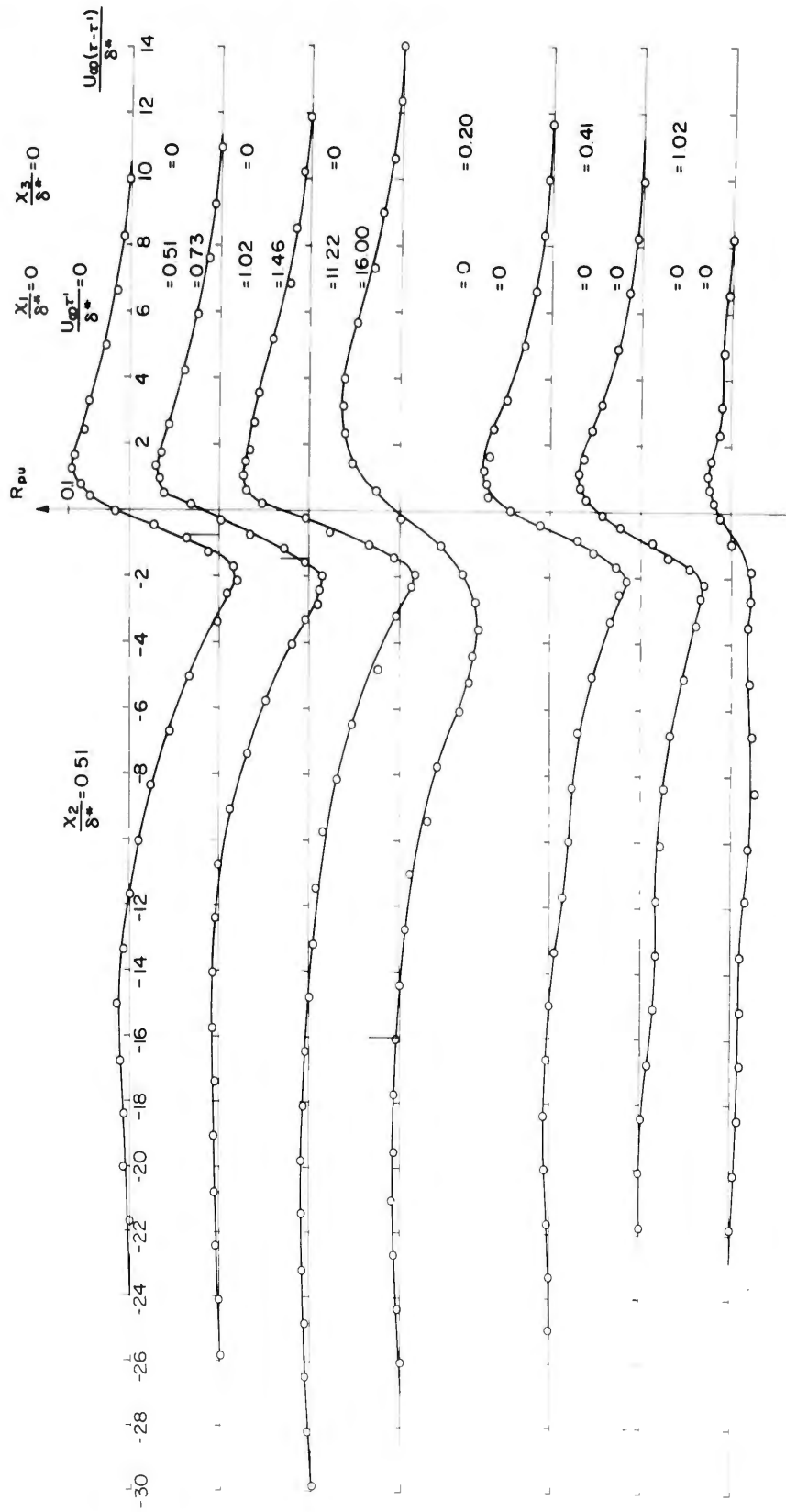


Fig. 13 Measured values of the space-time correlation of fluctuating velocity with fluctuating wall pressure

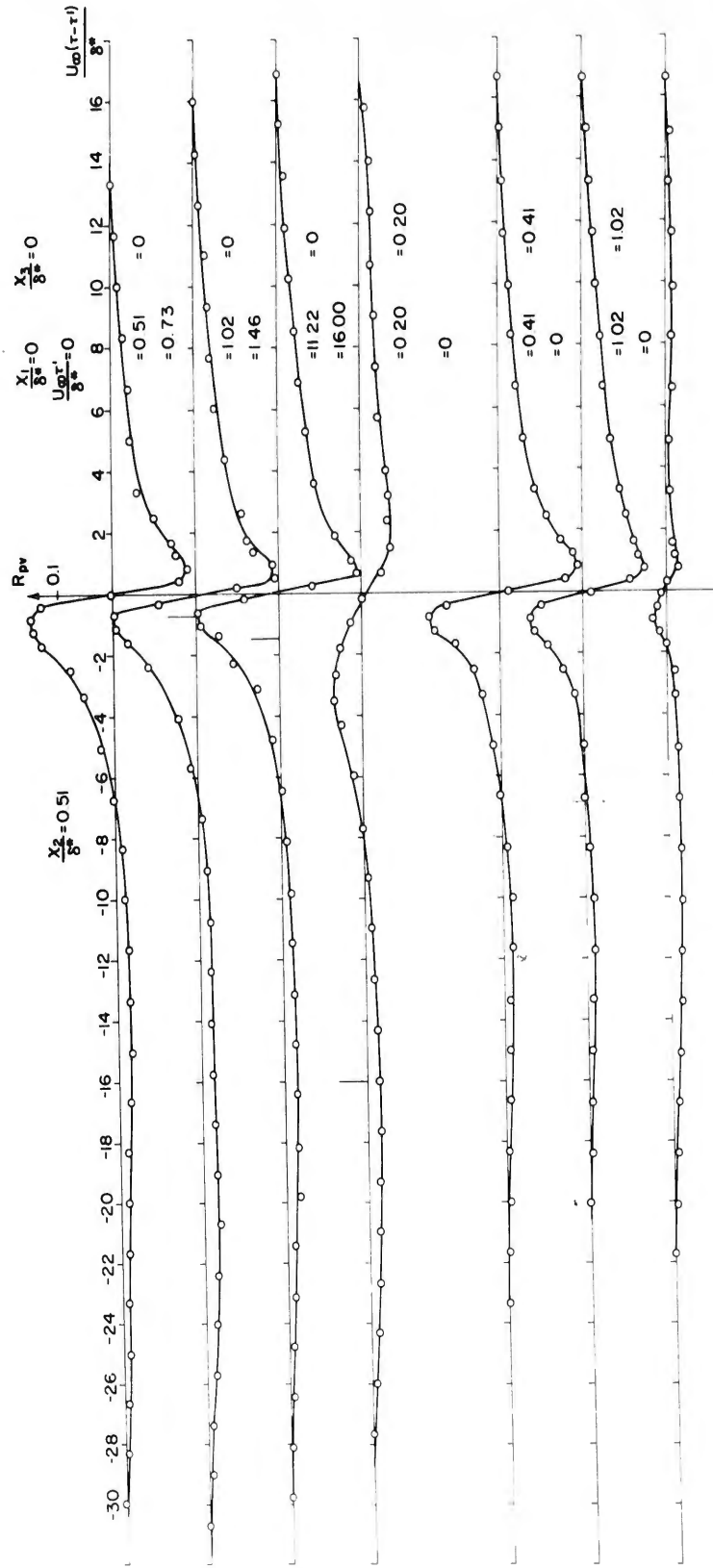


Fig. 14 Measured values of the space-time correlation of fluctuating velocity with fluctuating wall pressure

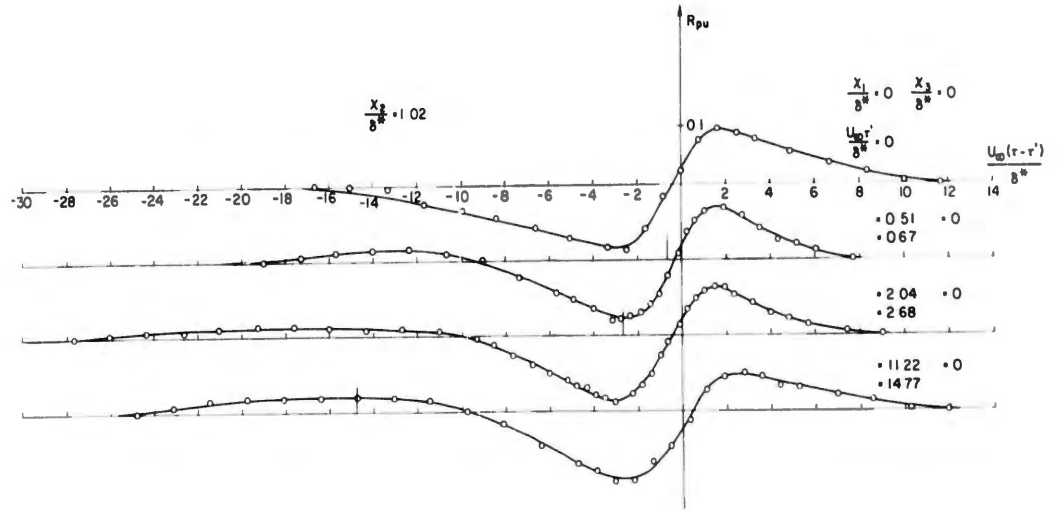


Fig.15 Measured values of the space-time correlation of fluctuating velocity with fluctuating wall pressure

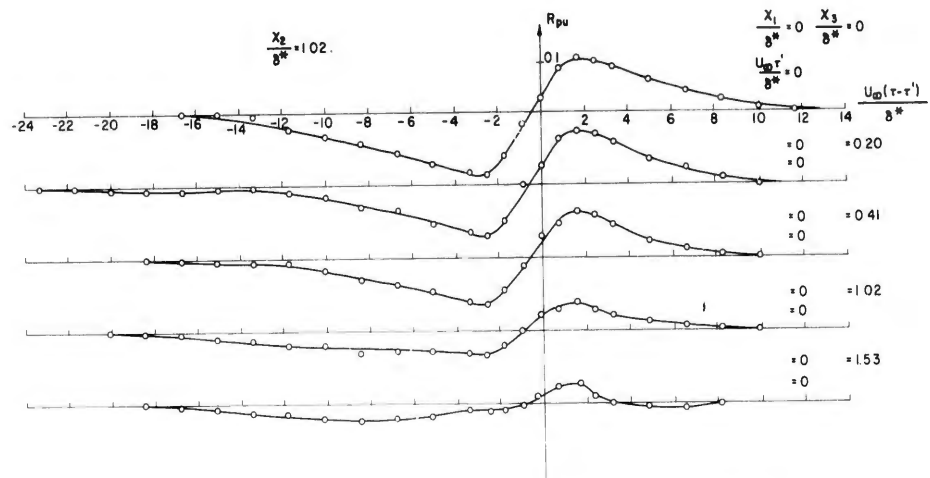


Fig.16 Measured values of the space-time correlation of fluctuating velocity with fluctuating wall pressure

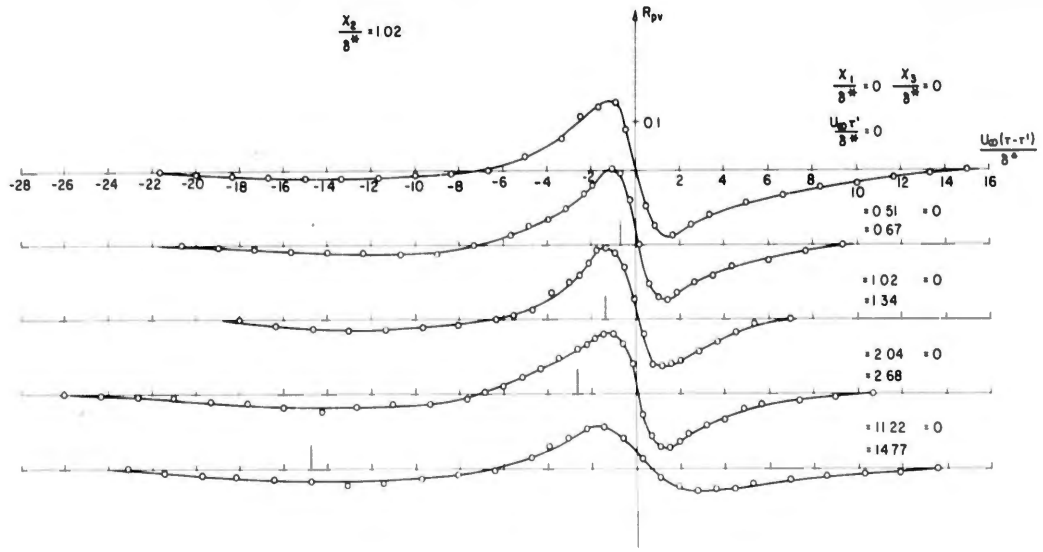


Fig.17 Measured values of the space-time correlation of fluctuating velocity with fluctuating wall pressure

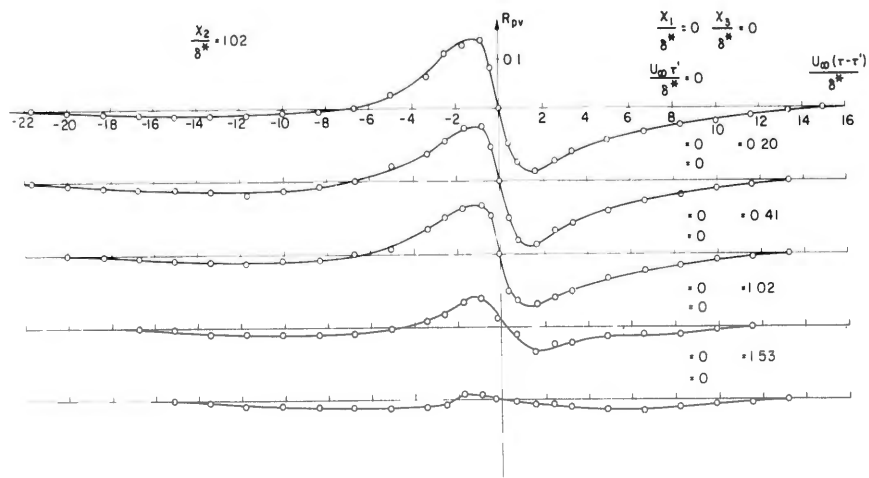


Fig.18 Measured values of the space-time correlation of fluctuating velocity with fluctuating wall pressure

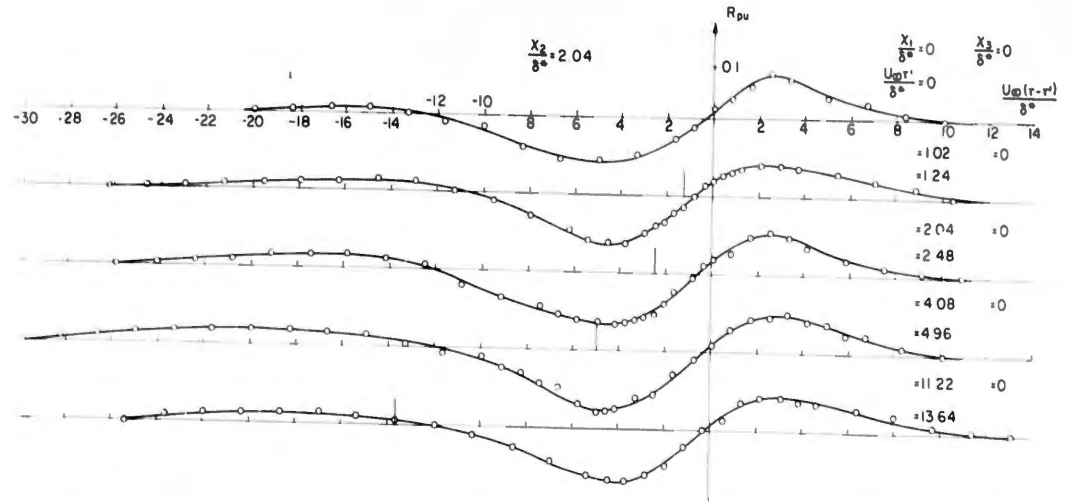


Fig.19 Measured values of the space-time correlation of fluctuating velocity with fluctuating wall pressure

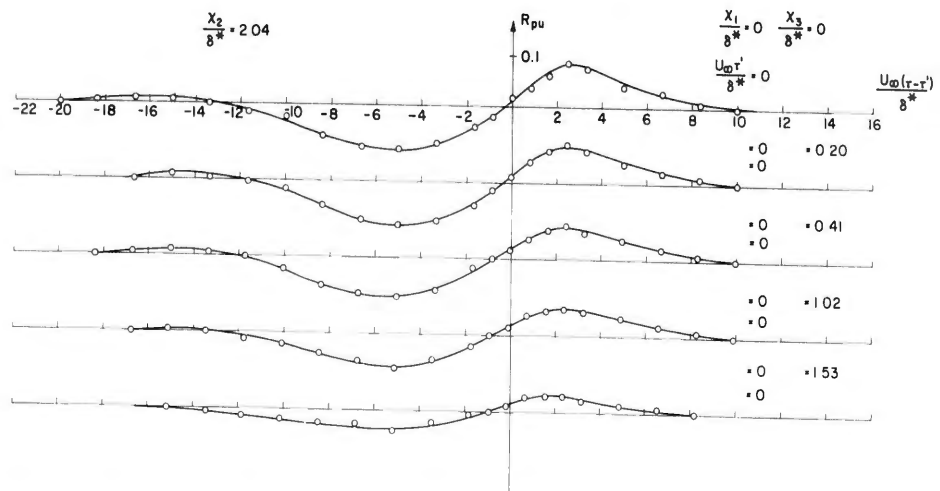


Fig.20 Measured values of the space-time correlation of fluctuating velocity with fluctuating wall pressure

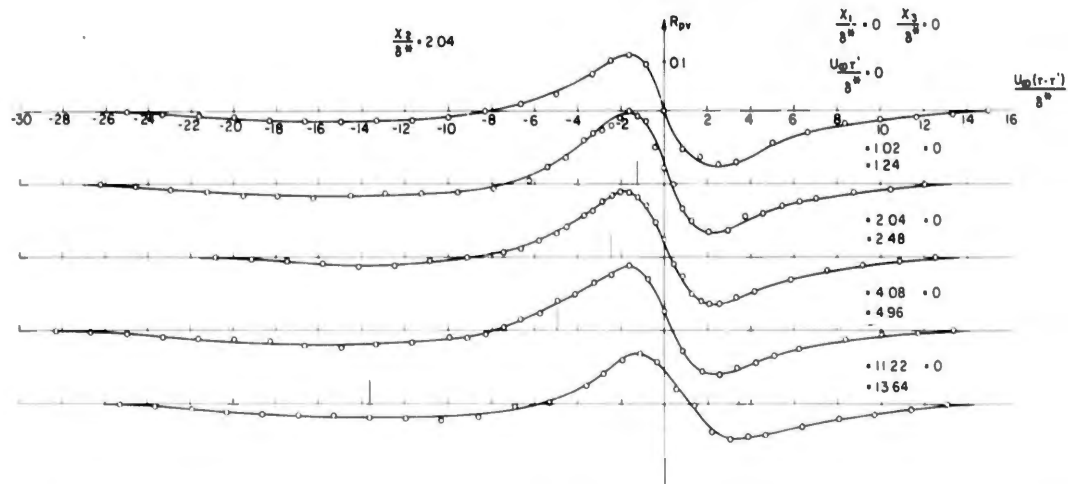


Fig.21 Measured values of the space-time correlation of fluctuating velocity with fluctuating wall pressure

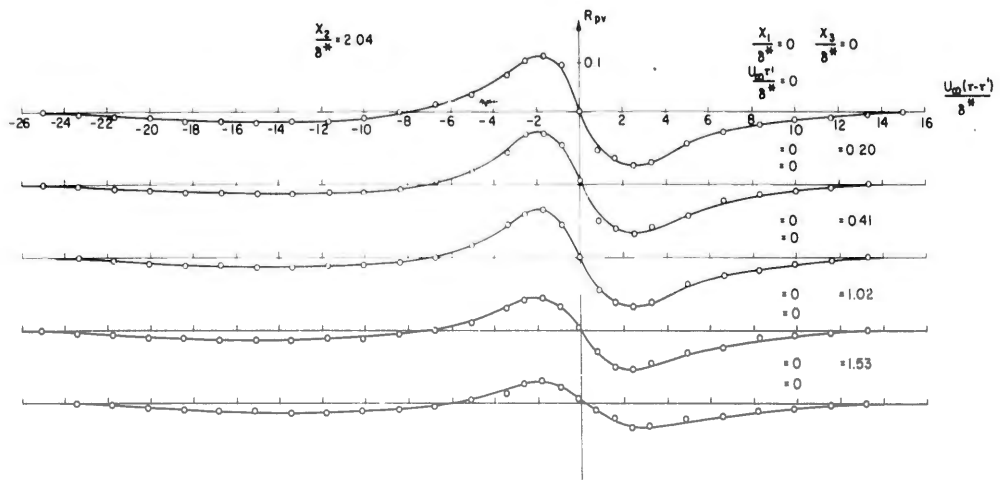


Fig.22 Measured values of the space-time correlation of fluctuating velocity with fluctuating wall pressure

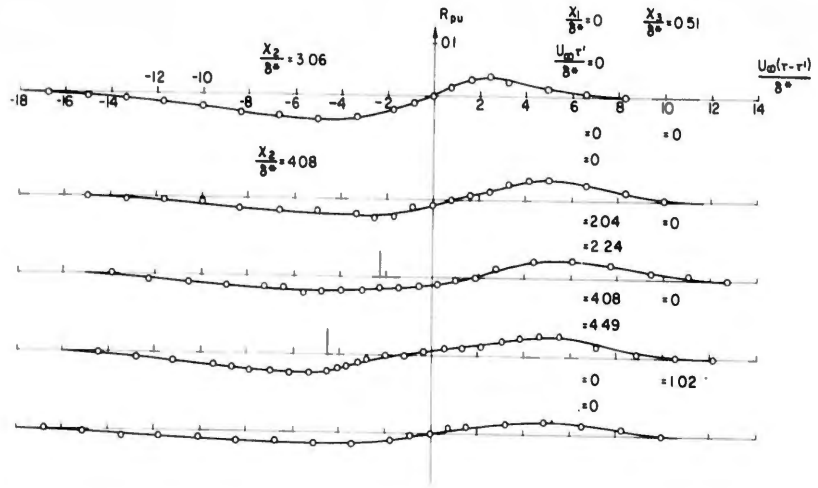


Fig.23 Measured values of the space-time correlation of fluctuating velocity with fluctuating wall pressure

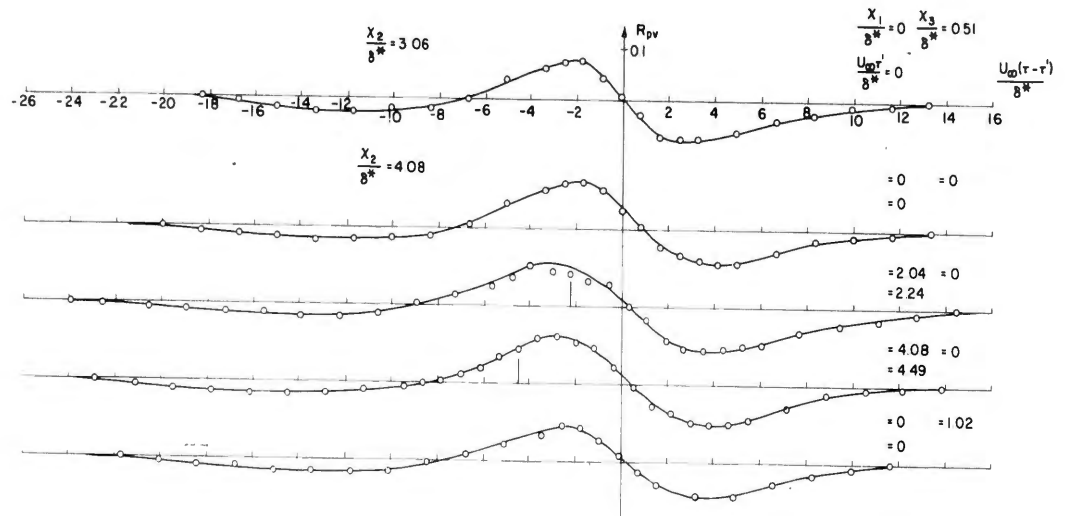


Fig.24 Measured values of the space-time correlation of fluctuating velocity with fluctuating wall pressure

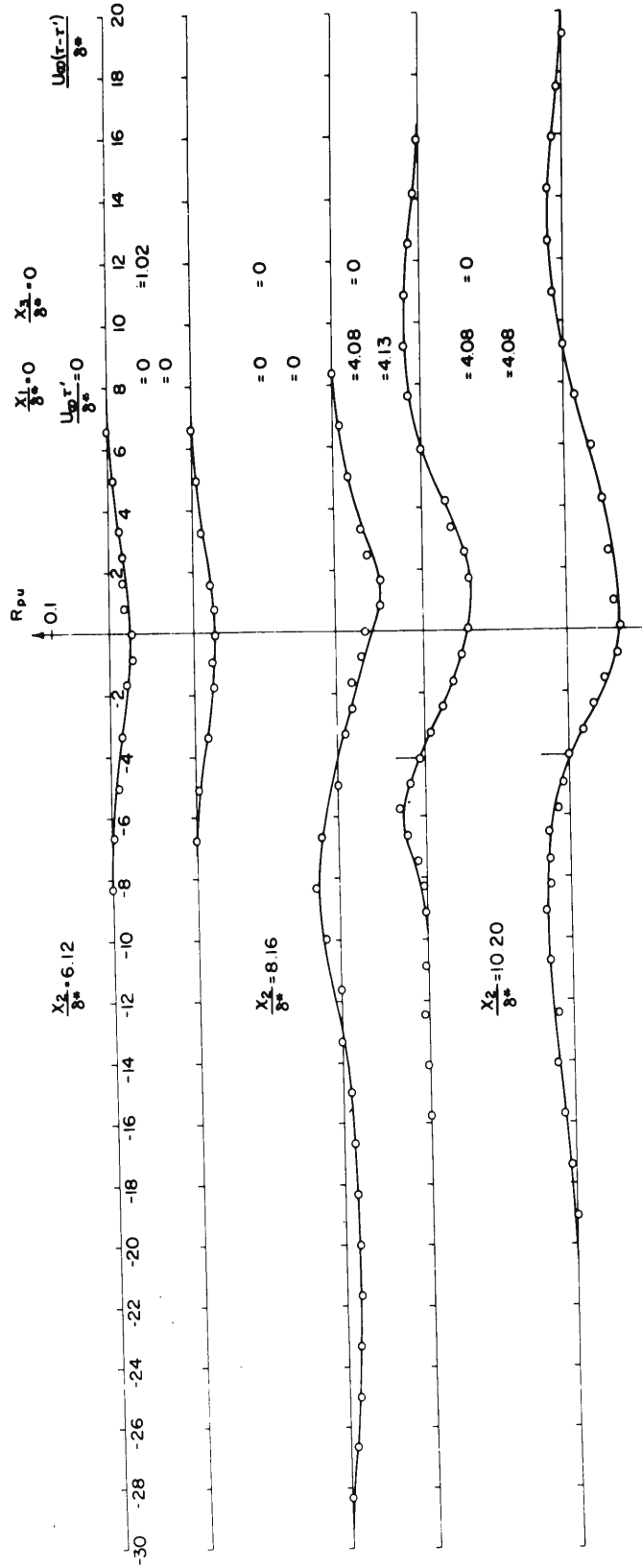


Fig. 25 Measured values of the space-time correlation of fluctuating velocity with fluctuating wall pressure

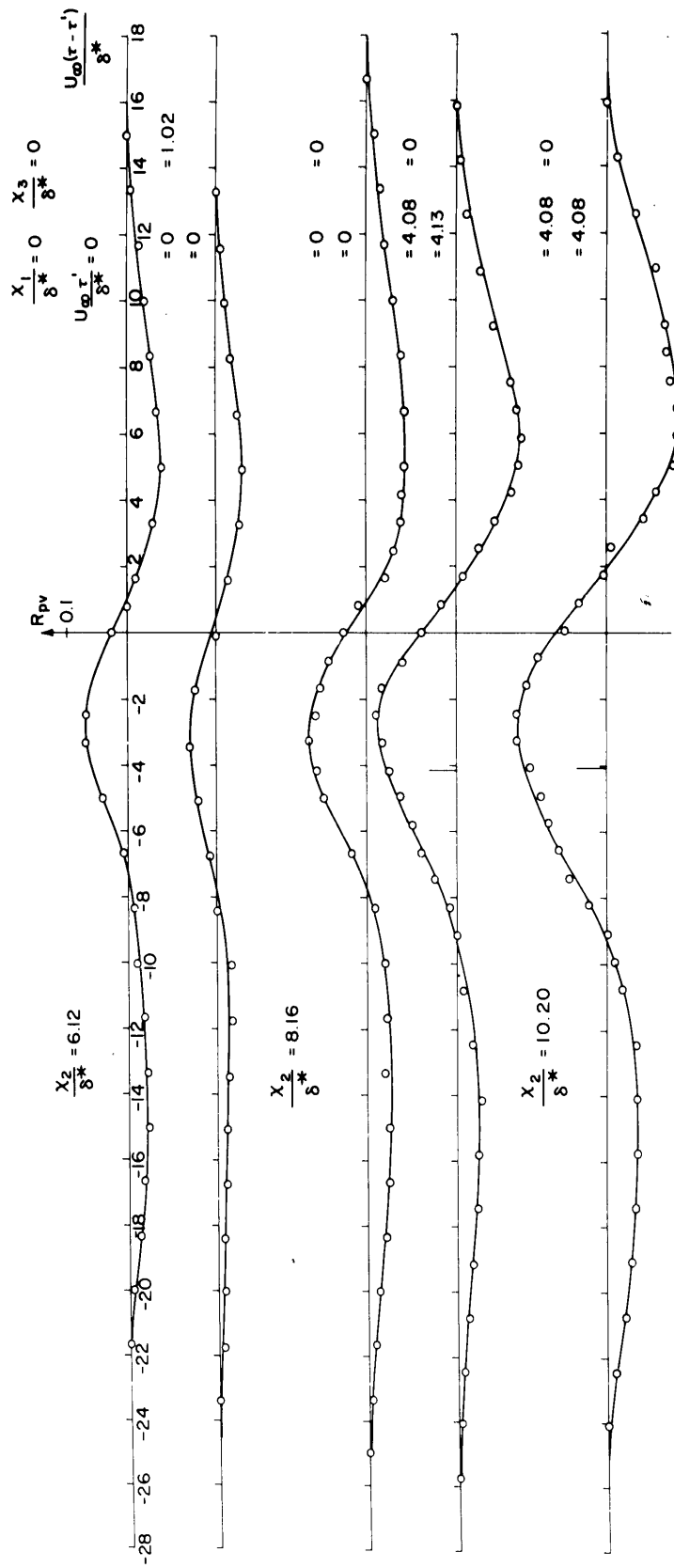


Fig. 26 Measured values of the space-time correlation of fluctuating velocity with fluctuating wall pressure

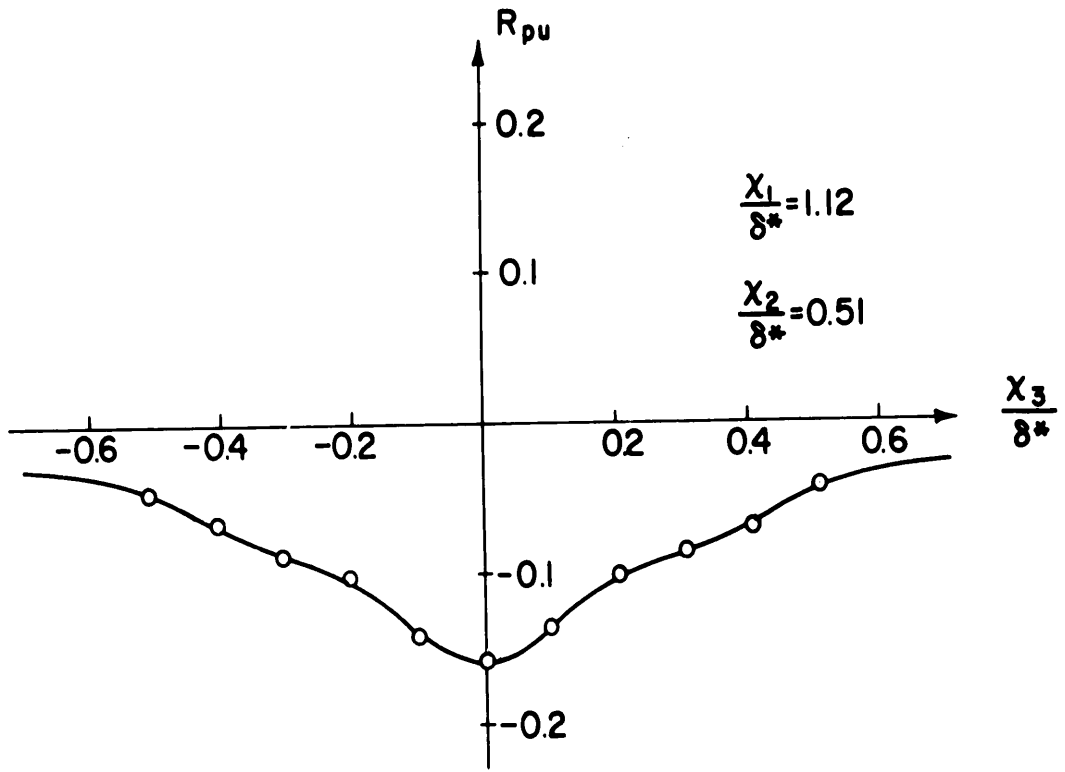


Fig. 27 Measured values of the spatial correlation of fluctuating longitudinal velocity with fluctuating wall pressure showing symmetry in the transverse direction

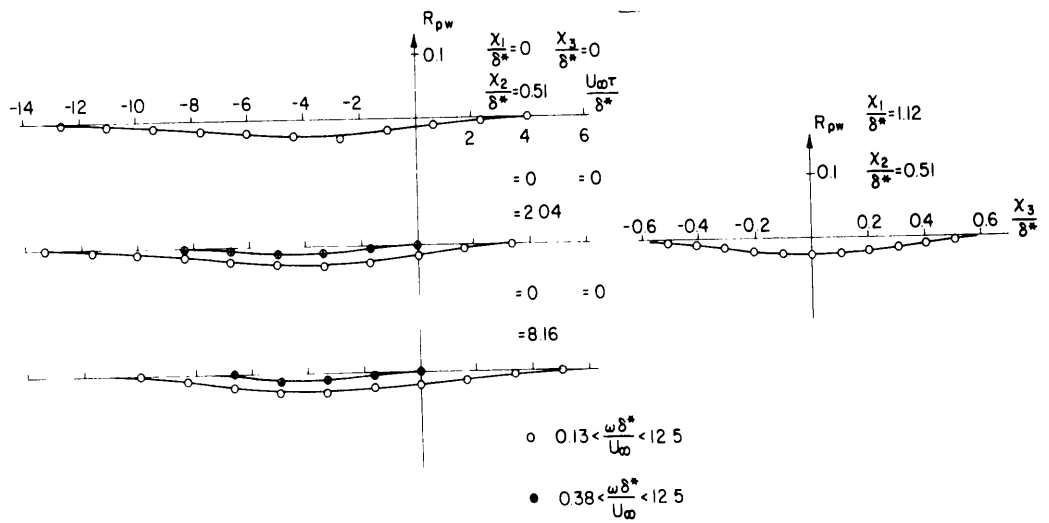


Fig. 28 Measured values of the space-time correlations of fluctuating transverse velocity with fluctuating wall pressure showing the effect of extraneous large-scale flow disturbance probably caused by Taylor-Goertler vortices and density stratification

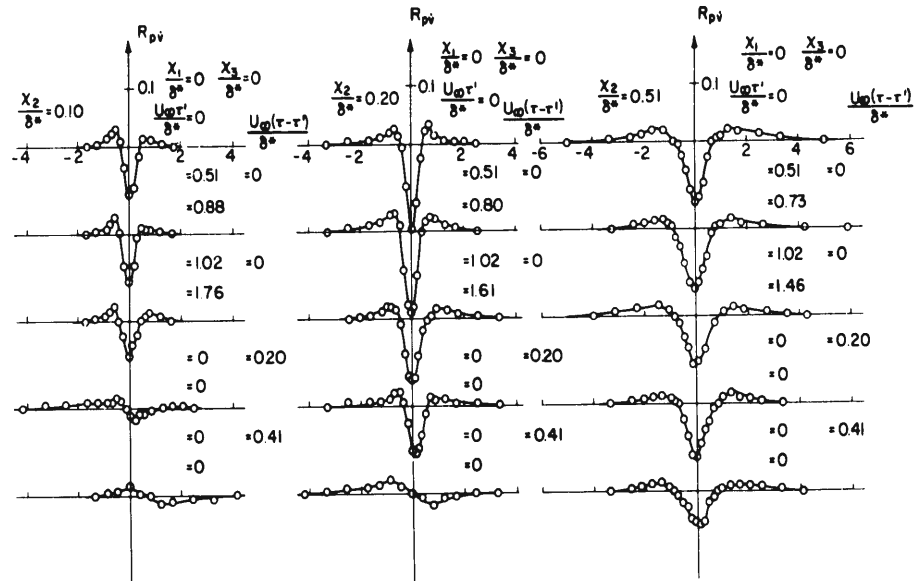


Fig. 29 Measured values of the space-time correlation of the time derivative of fluctuating velocity normal to the wall with fluctuating wall pressure

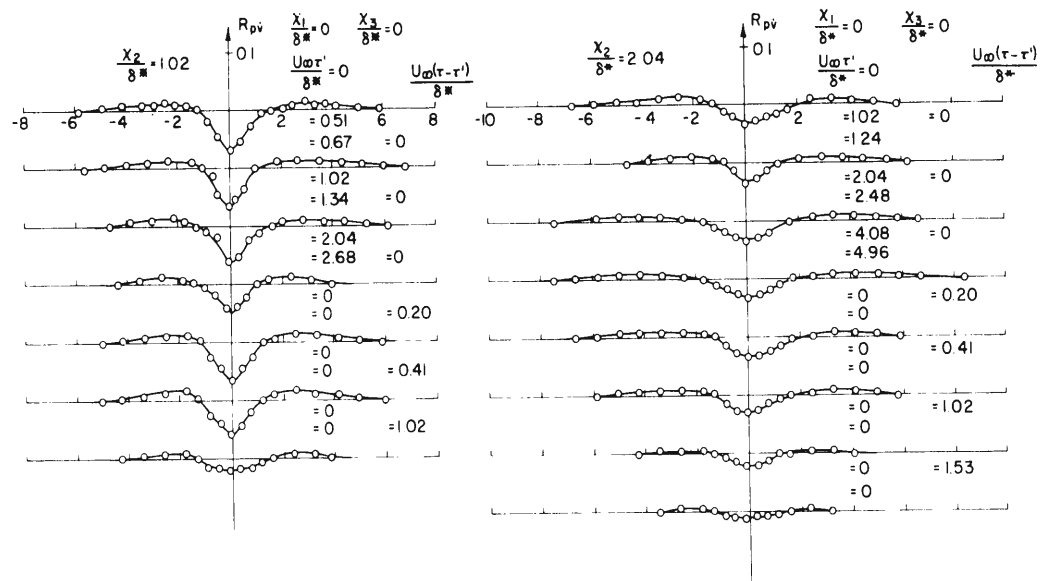


Fig. 30 Measured values of the space-time correlation of the time derivative of fluctuating velocity normal to the wall with fluctuating wall pressure

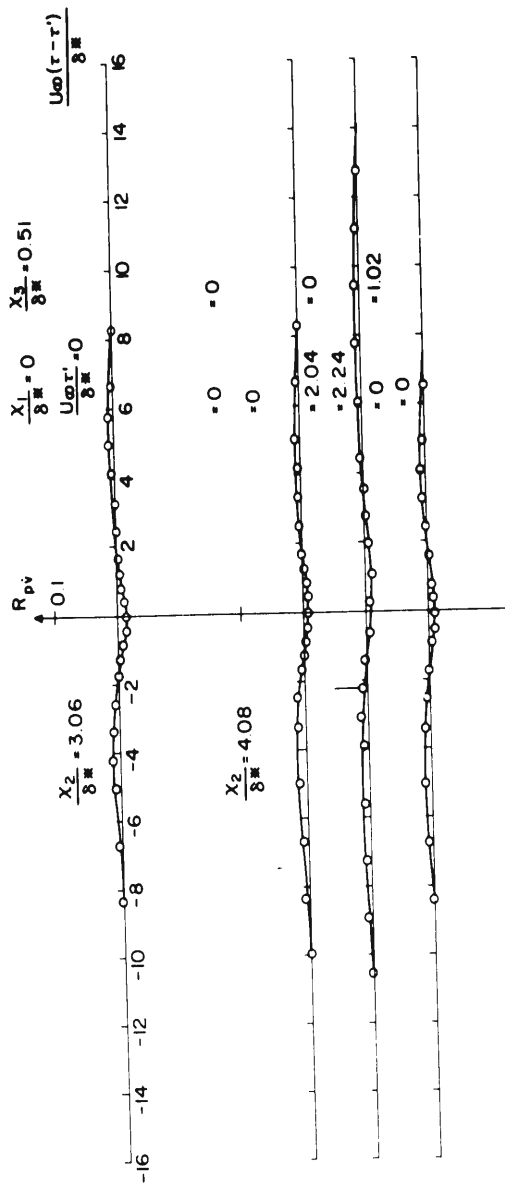


Fig. 31 Measured values of the space-time correlation of the time derivative of fluctuating velocity normal to the wall with fluctuating wall pressure

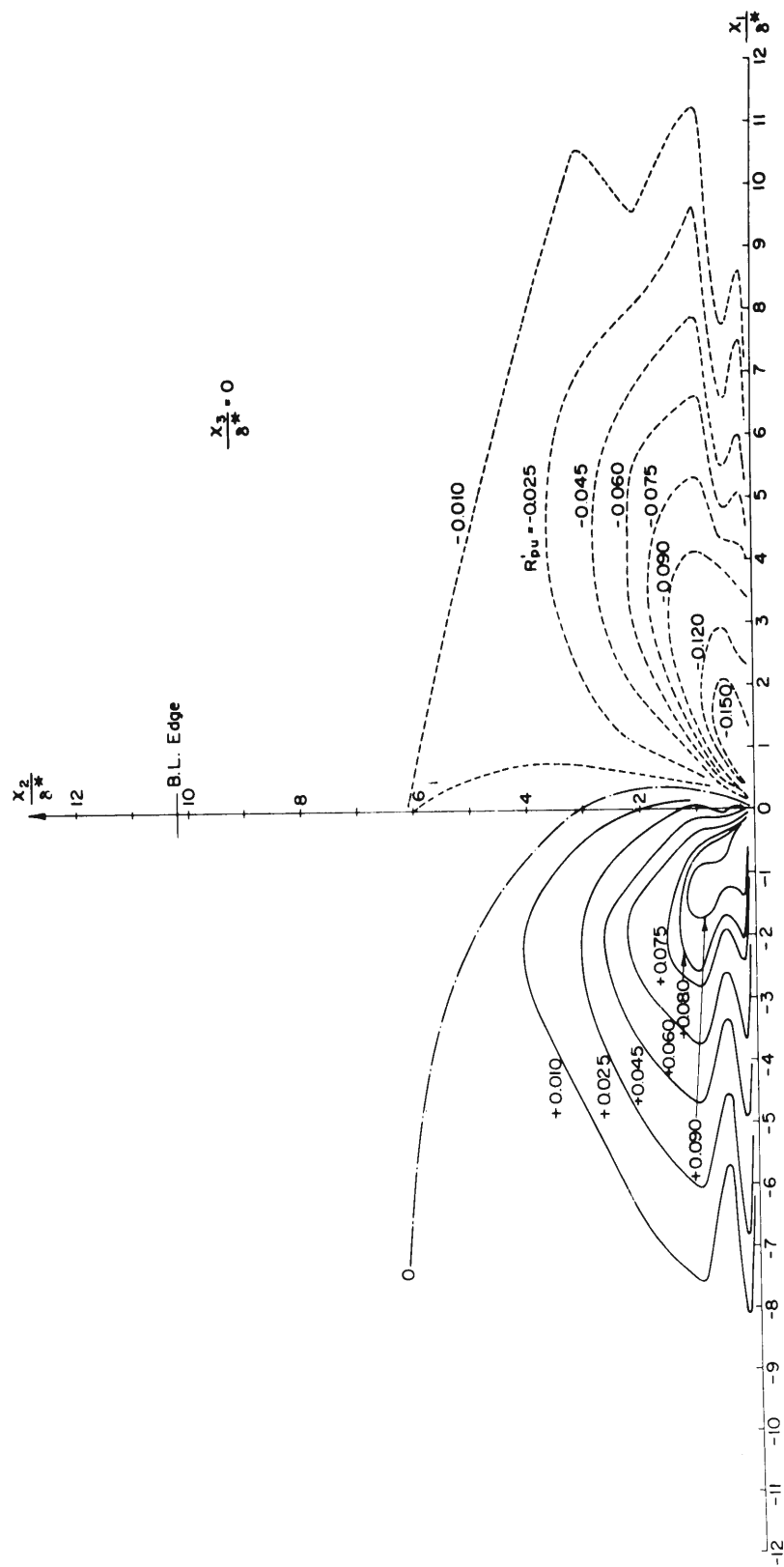


Fig. 32 Correlation contours of R'_{pu} in the x_1 - x_2 plane. Correlation normalized on the value of the velocity fluctuation at $x_2/\delta^* = 0.51$. Origin of coordinate system at pressure transducer

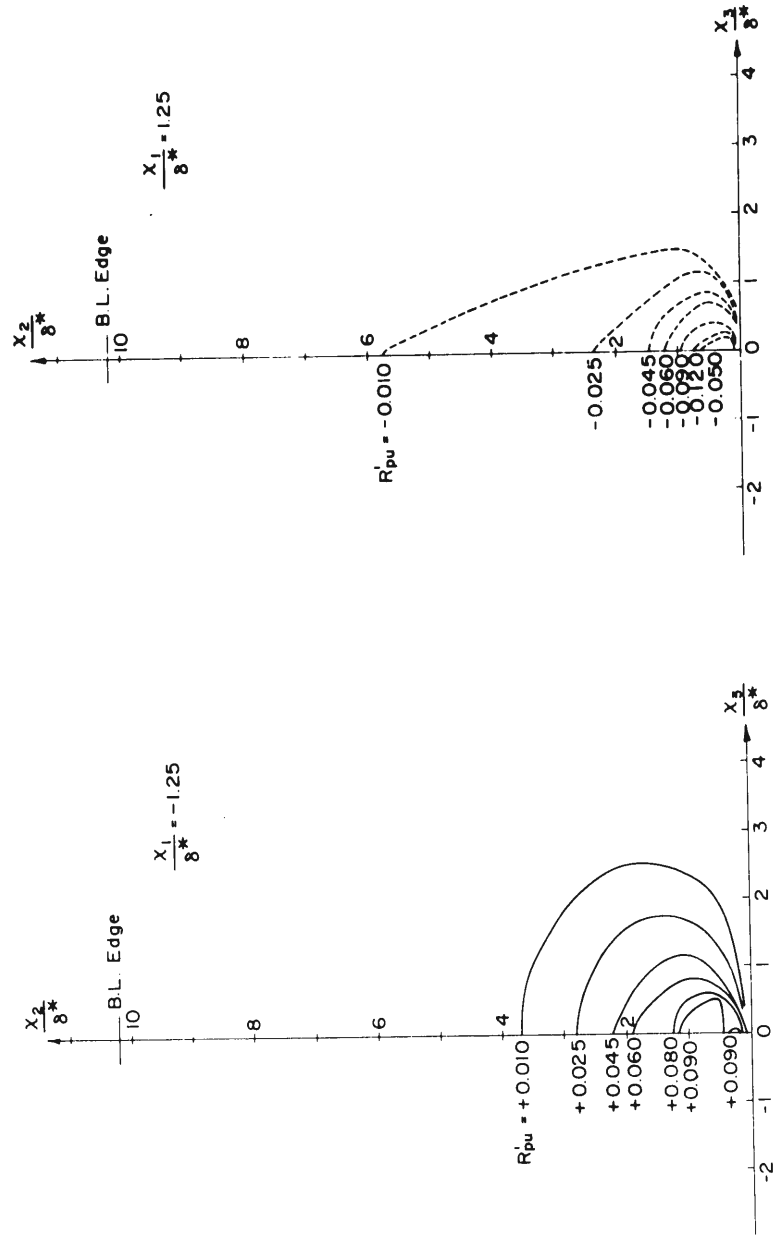


Fig. 33 Correlation contours of R'_{pu} in the x_2 - x_3 plane. Correlation normalized on the value of the velocity fluctuation at $x_2/\delta^* = 0.51$. Origin of coordinate system at pressure transducer

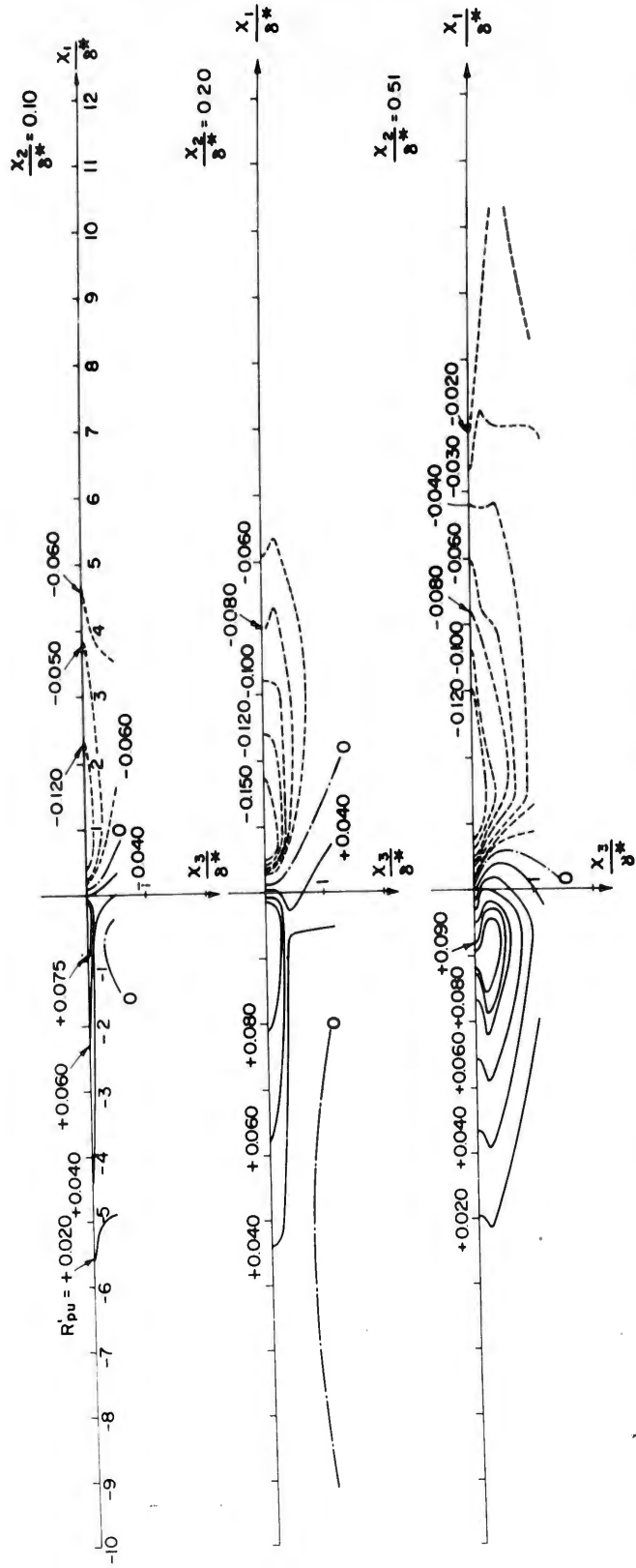


Fig. 34 Correlation contours of R'_{pu} in the x_1-x_3 plane. Correlation normalized on the value of the velocity fluctuation at $x_2/\delta^* = 0.51$. Origin of coordinate system at pressure transducer

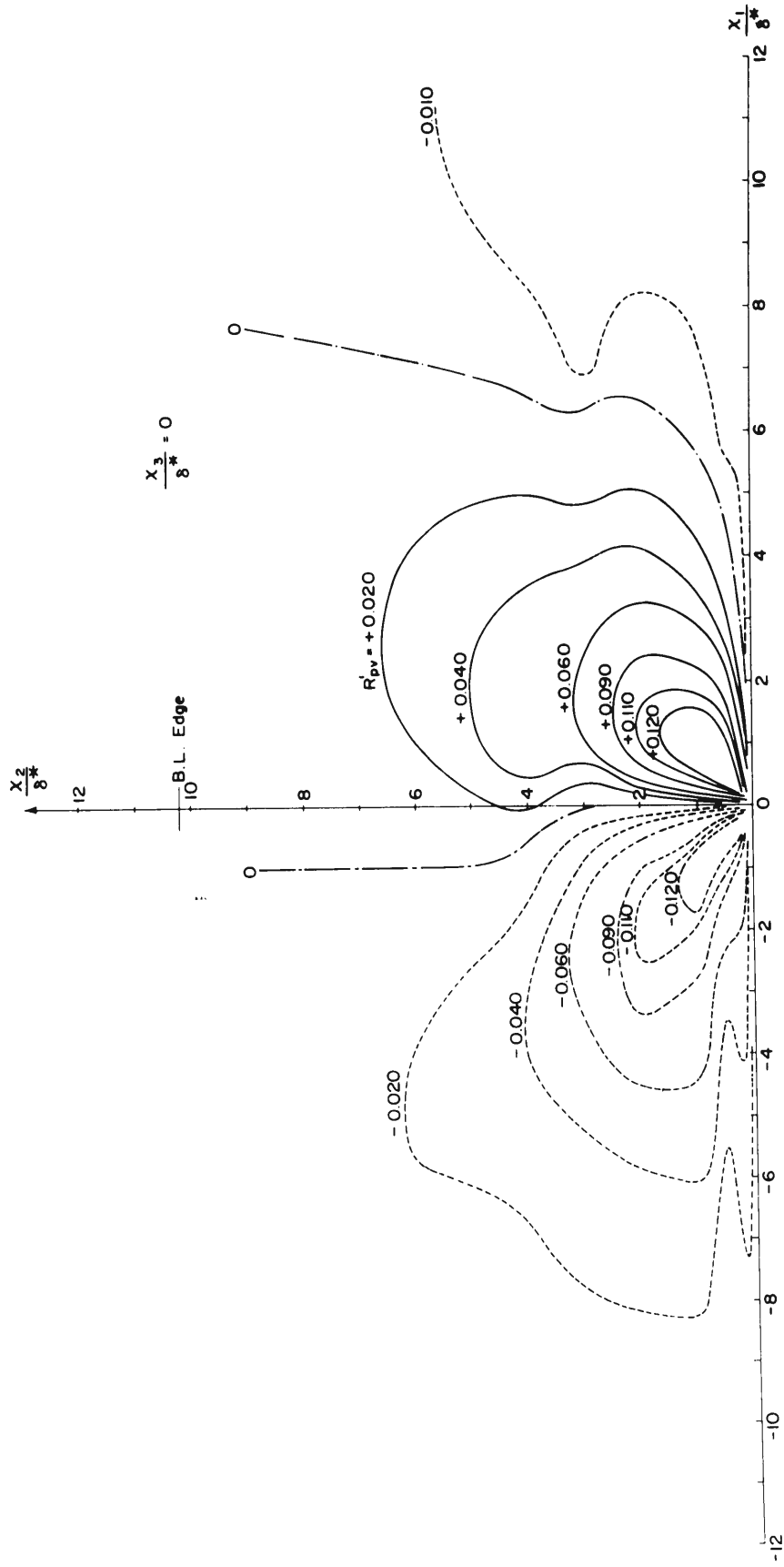


Fig. 35 Correlation contours of R'_{pv} in the x_1 - x_2 plane. Correlation normalized on the value of the velocity fluctuation at $x_p/\delta^* = 0.51$. Origin of coordinate system at pressure transducer

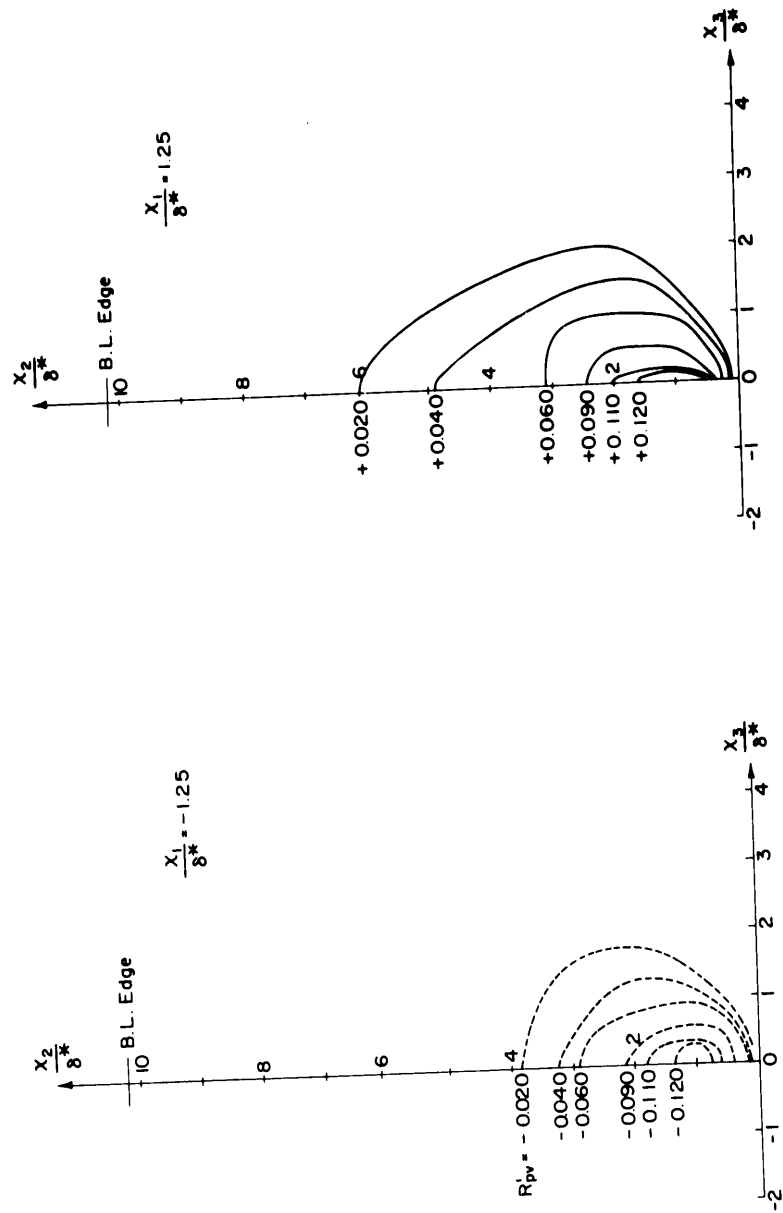


Fig. 36 Correlation contours of R'_{pv} in the x_2-x_3 plane. Correlation normalized on the value of the velocity fluctuation at $x_2/\delta^* = 0.51$. Origin of coordinate system at pressure transducer

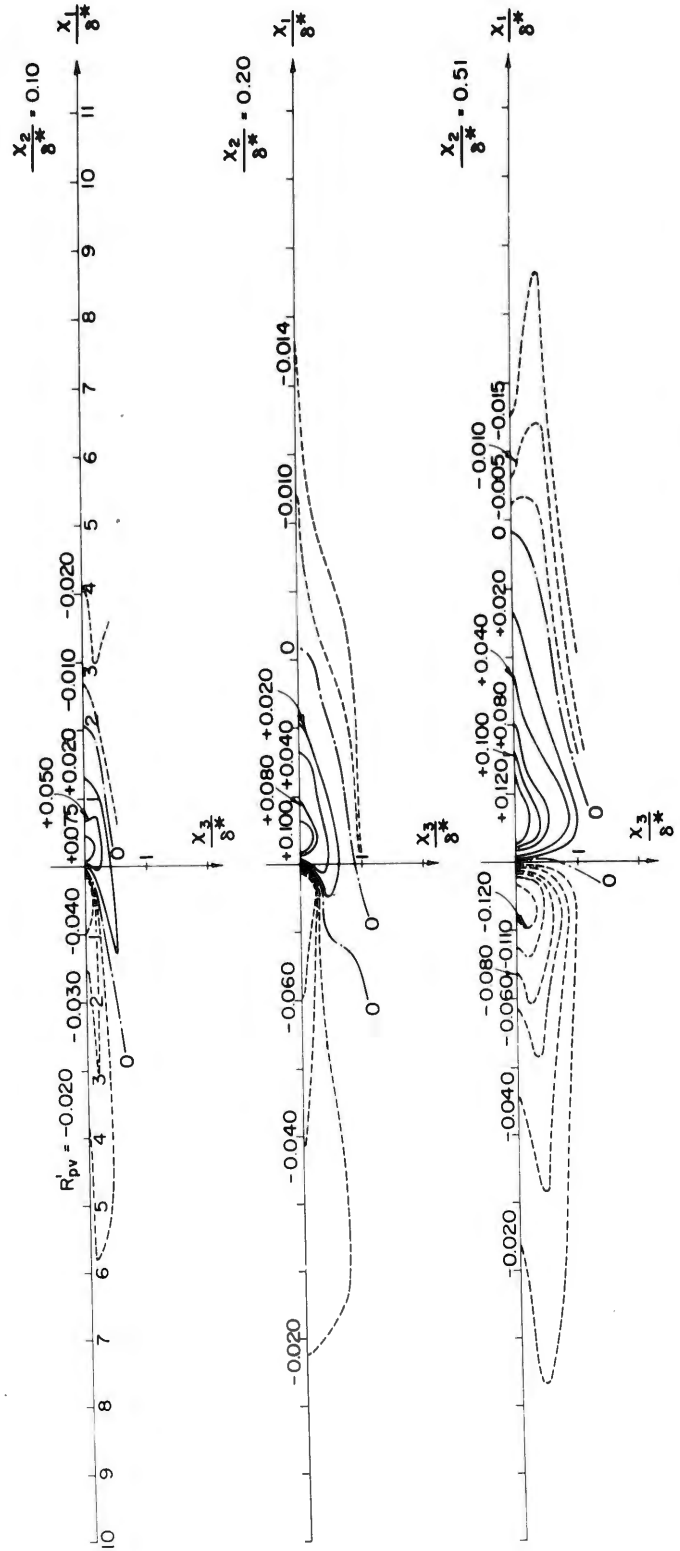


Fig. 37 Correlation contours of R'_{pv} in the x_1-x_3 plane. Correlation normalized on the value of the velocity fluctuation at $x_2/\delta^* = 0.51$. Origin of coordinate system at pressure transducer

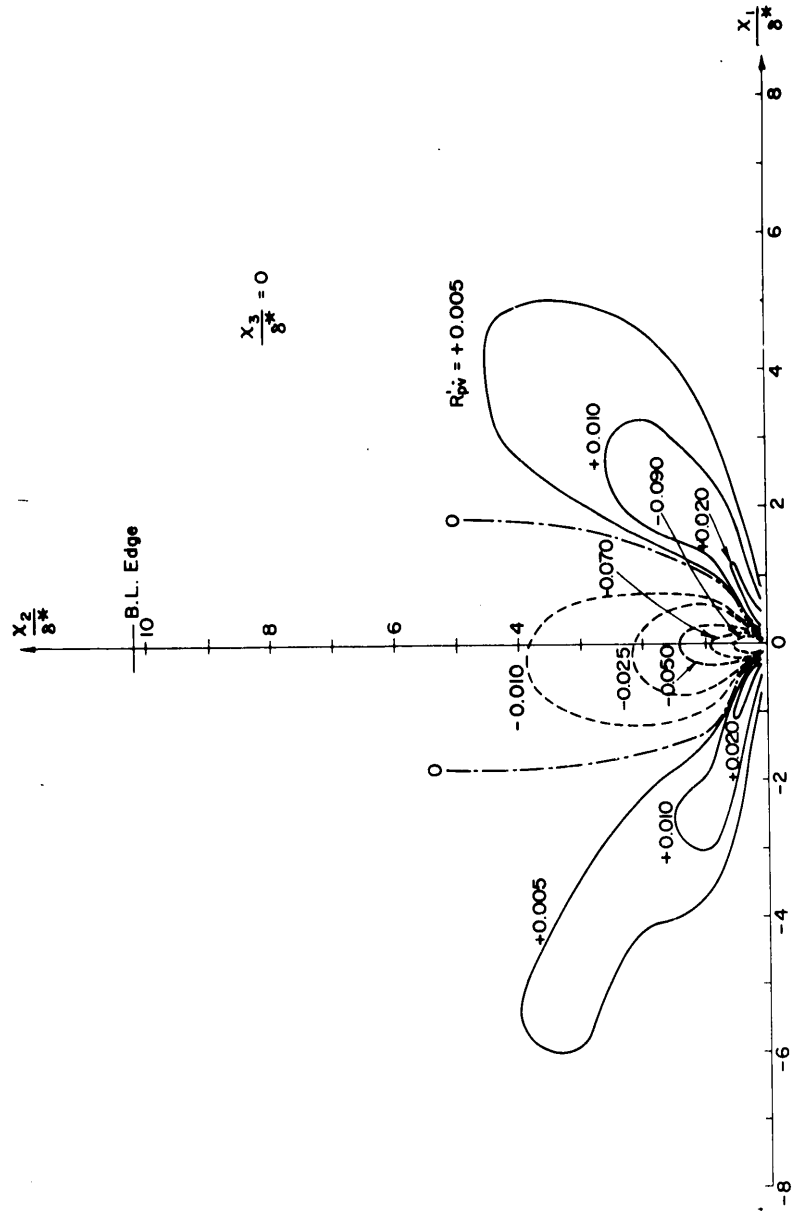


Fig. 38 Correlation contours of $R'_{v'v'}$ in the x_1 - x_2 plane. Correlation normalized on the value of the velocity fluctuation derivative at $x_2/\delta^* = 0.51$.
Origin of coordinate system at pressure transducer

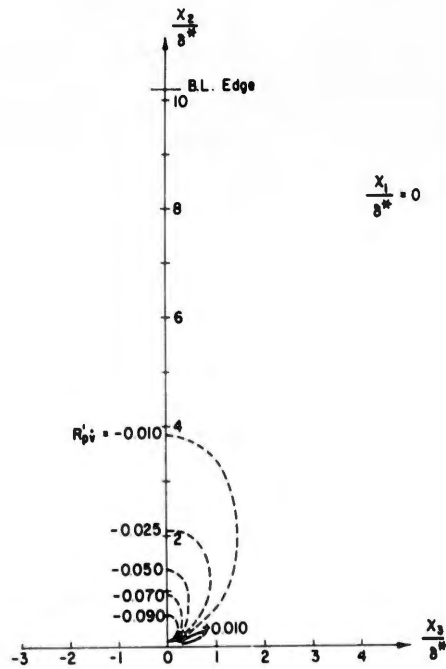


Fig. 39 Correlation contours of R'_{pv} in the x_2 - x_3 plane. Correlation normalized on the value of the velocity fluctuation derivative at $x_2/\delta^* = 0.51$.
Origin of coordinate system at pressure transducer

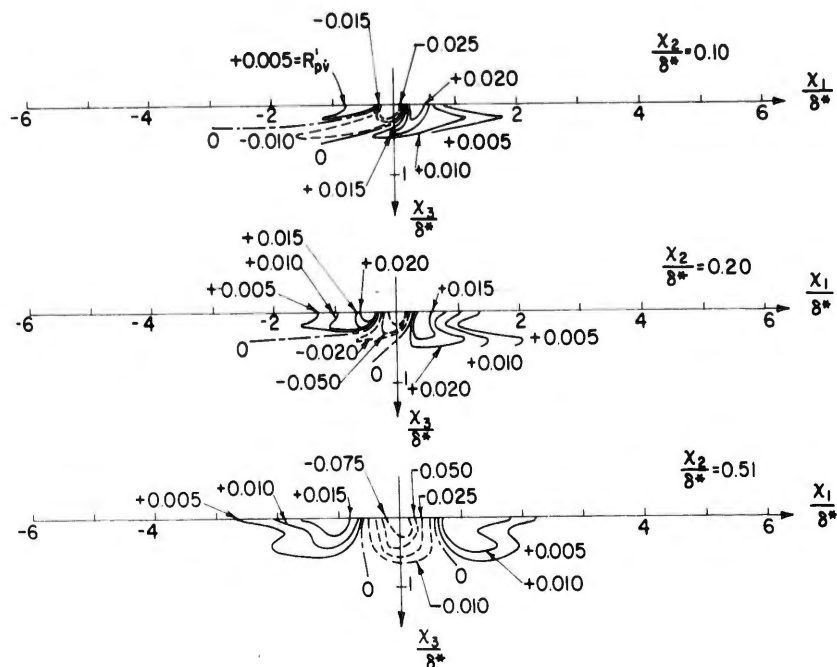


Fig. 40 Correlation contours of R'_{pv} in the x_1 - x_3 plane. Correlation normalized on the value of the velocity fluctuation derivative at $x_2/\delta^* = 0.51$.
Origin of coordinate system at pressure transducer

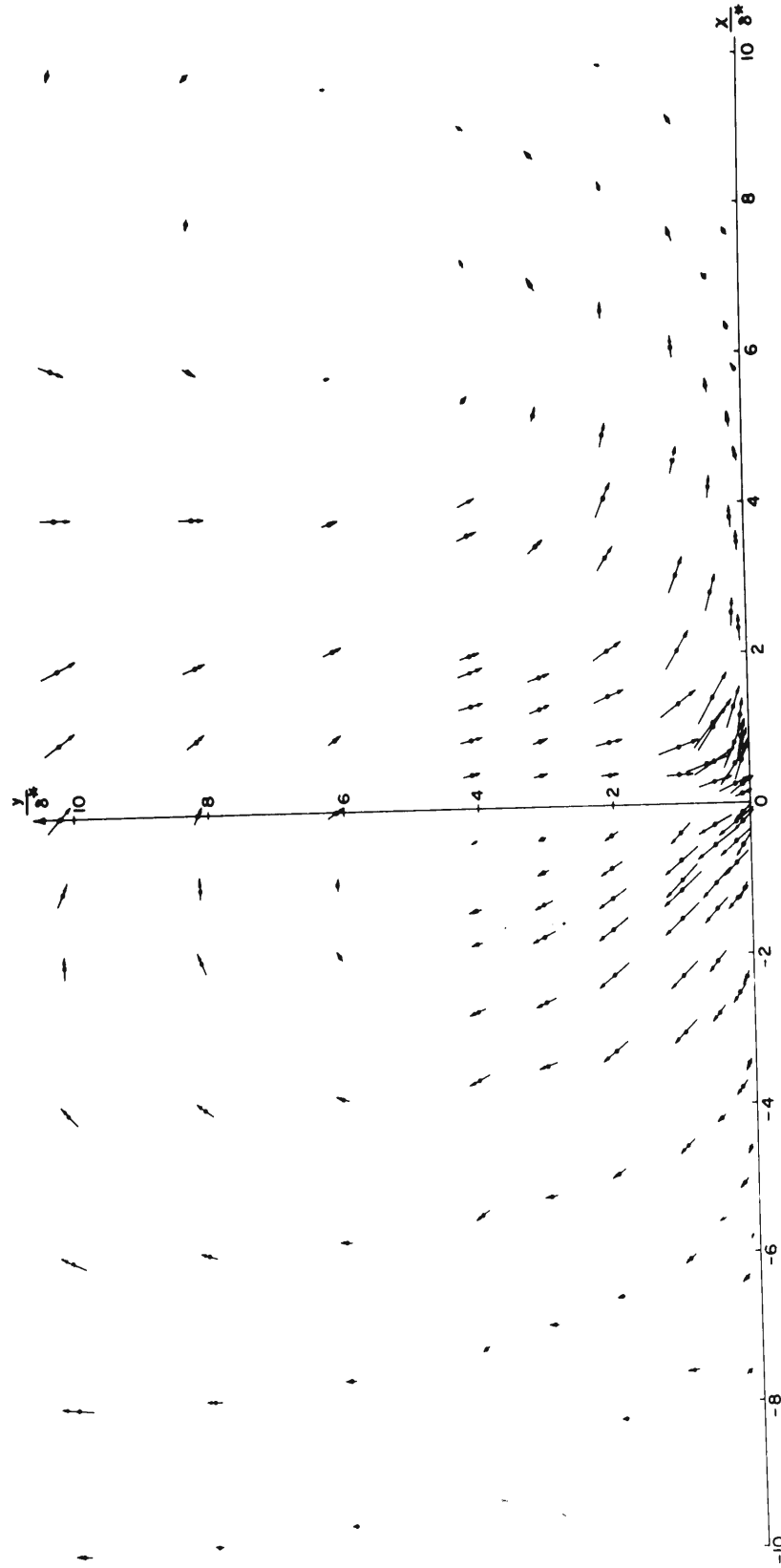


Fig. 41 Vector field of correlation. Magnitude of the vector at any point is $\sqrt{(R_{pu}^2 + R_{pv}^2)}$. Direction of the vector at any point as measured from the positive x_1 -axis is given by $\tan^{-1} \frac{R_{pv}}{R_{pu}}$

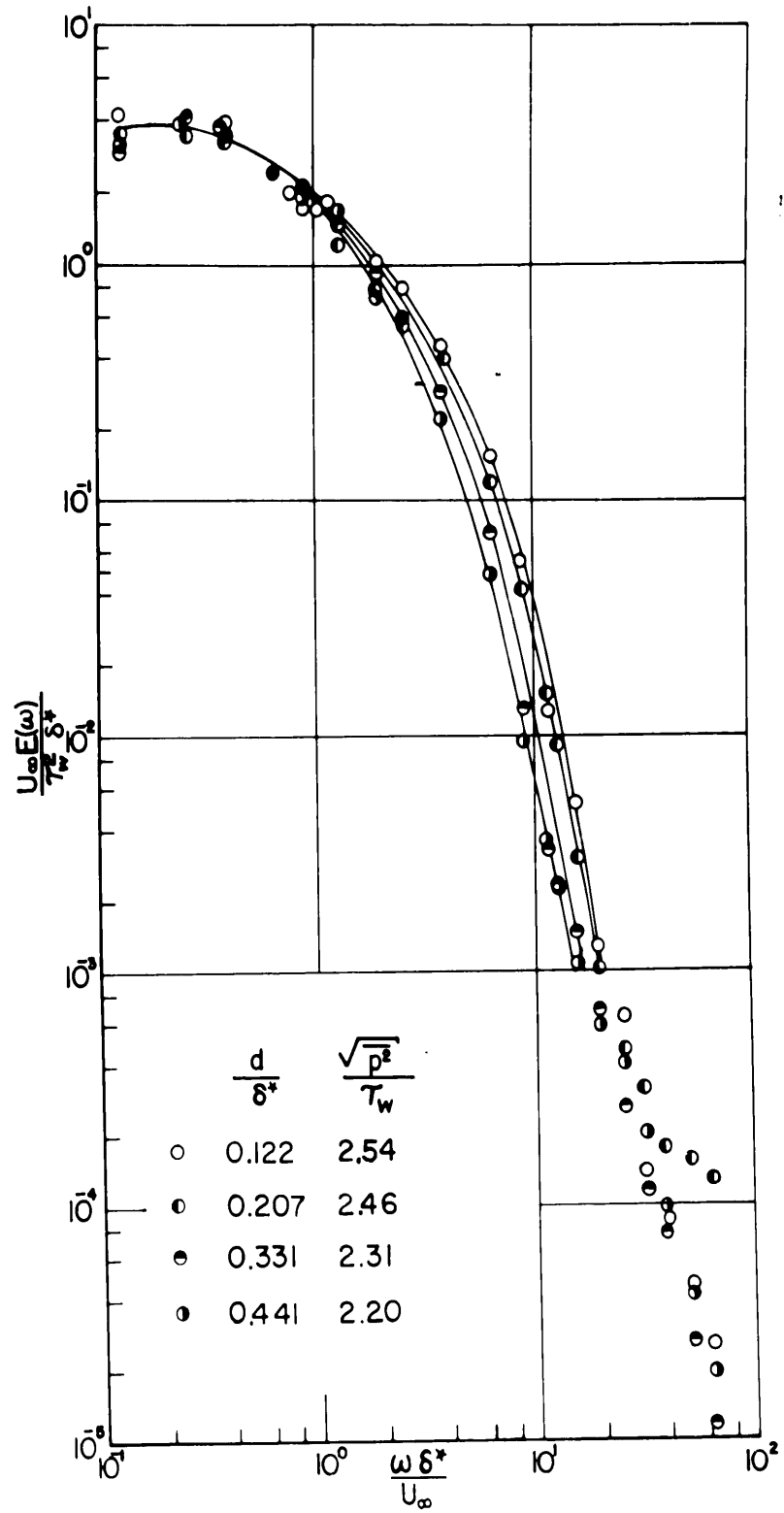


Fig. 42 Dimensionless power spectrum of the wall pressure measured by four different size transducers

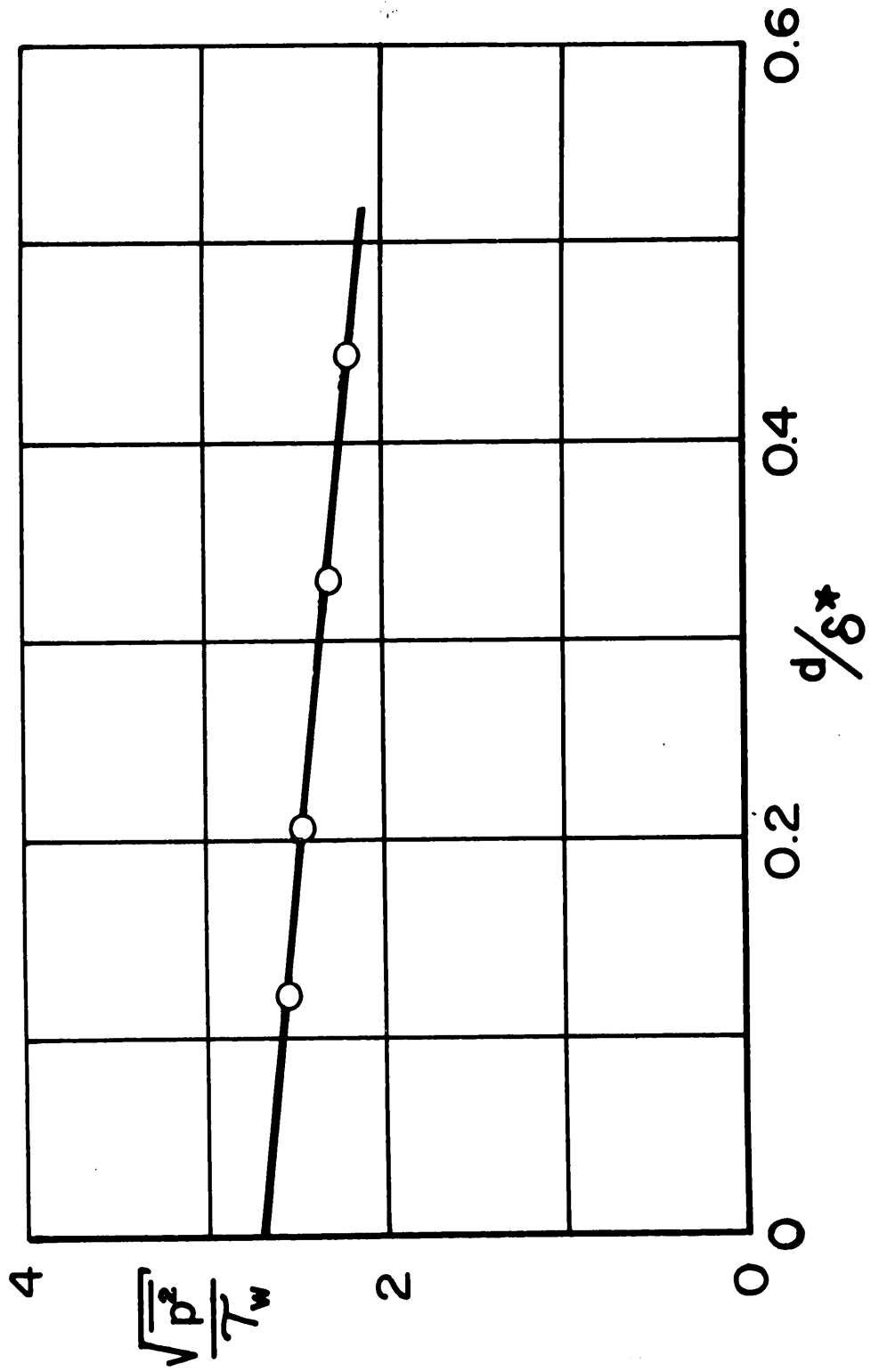


Fig. 43 Dimensionless root-mean-square wall pressure computed from area under faired curves of Figure 42

APPENDIX

The spectrum of the wall pressure has been remeasured with four different-diameter lead zirconate pressure transducers. The transducer construction has been described elsewhere¹⁵. The transducer sensitivity was determined by subjecting each transducer to a known sinusoidal pressure generated by an oscillating piston whose diameter and amplitude of oscillation were measured. The frequency response of the transducers was not checked but is presumed to be flat in the range of interest $1 < f < 50,000$ cycles/sec because our previous transducers¹⁵, made in the same way, had a flat frequency response.

The measured spectra are shown in Figure 42. It is apparent that at dimensionless frequencies above $\frac{\omega \delta^*}{U_\infty} \approx 1$ the smaller diameter transducers measured a larger spectral density. This is the effect of the finite transducer diameter which affects the resolving power of the instrument.

Uberoi and Kovaszny²¹ have given the general method for correcting measurements made with instruments of inadequate resolving power. In order to use the method correctly, one must measure the complete correlation field of the wall pressure or the complete cross spectral density of the wall pressure with the finite size transducer. In principle, the correct wall pressure correlation field or cross spectral density may then be computed. In actual practice, it will always be impossible to recover all the information because the smallest scale signals are severely attenuated and will be submerged by unavoidable noise. Thus, the correction method may be used up to a certain point where the signal to noise ratio becomes too small. Beyond that point the corrected spectral density is too large.

Corrections of the wall pressure spectra have been attempted by one of us²², but were not successful because the space-time correlations were not completely known at that time. Since then, Corcos²³ has attempted to apply our later space-time correlation measurements to the spectra, but he had to assume a relation for the dependence of the pressure correlation on x_3 and τ . Corcos also made an unnecessary simplifying assumption in his correction method.

We have not attempted to correct our spectra but would rather state that the correct spectra for a transducer of zero diameter is not very much different from that measured by our smallest transducer (see Fig. 46).

By extrapolation of the spectral density at each frequency to the spectral density that would be measured by a vanishingly small transducer, we have constructed the spectrum that would be measured by an infinite small transducer and then computed the ratio of the areas under the extrapolated spectrum and the spectrum measured by the smallest transducer ($\frac{d}{\delta^*} = 0.122$) and we find that the ratio is 1.1.

Therefore, the smallest transducer measures a root-mean-square wall pressure that is only 5 per cent too low. The extrapolated value of the root-mean-square pressures are shown in Figure 47. It can be observed that the scatter of the spectra data is

considerable at low frequencies in Figure 46. We have computed the mean-square pressures of Figure 47 from the area under the faired curves of Figure 46. The low frequency disturbances were caused by disturbances in the wind tunnel. Some are sound from the diffuser and some are presumably large scale eddies in the tunnel.

The root-mean-square pressure and spectra for the transducer with $\frac{d}{\delta^*} = 0.331$, that were used in the body of this Report, are lower than those measured and reported in this Appendix. $\sqrt{\overline{p^2}}/\tau_w = 2.64$ was the value that we measured previously (see Section 3.2.2). When the present tests with four different transducers were made, we took great care to smooth the floor of the tunnel and aligned the large plate carrying the transducers very carefully with the floor. The effect was immediately noticeable and reduced the root-mean-square pressure (and spectra) from $\sqrt{\overline{p^2}}/\tau_w = 2.64$ to $\sqrt{\overline{p^2}}/\tau_w = 2.31$. The lesson to be learned here is that quantitative measurements in turbulence are quite tedious and often difficult because the effect of extraneous disturbances that are hard to find and eliminate may be important.

DISCUSSION

G.M. Lilley

I would like to congratulate Professor Willmarth and Dr. Wooldridge on the excellence of their experimental data and the great use it will be to all workers in the field of pressure fluctuations in shear flows.

1. Could Professor Willmarth say whether he had checked his data, both filtered and unfiltered, against the strong boundary condition of Phillips which states that the surface integral of the wall pressure-velocity covariance in planes parallel with the wall must vanish if the disturbance outside the layer is zero?
2. Secondly, from the plotted values of $\overline{p(o)V}$, Willmarth and Wooldridge find that large values of this covariance exist near the outer edge of the boundary layer while values near the centre of the boundary layer are smaller. Has Professor Willmarth some explanations for this behaviour?
3. Thirdly, the data of Professors Willmarth and Wooldridge show that the magnitudes of $\overline{p(o)u}$, $\overline{p(o)v}$, $\overline{p(o)w}$ are all similar, and are presumably a reflection of the role of the pressure on the transference of energy among the different components of the turbulent velocity. Would Professor Willmarth like to comment?

Authors' reply

1. We have not checked our data, either filtered or unfiltered, against the surface integral condition of Phillips. A cursory examination of our filtered data on the pressure velocity covariance in a plane parallel to the wall shows that the condition appears to be approximately satisfied but we have not made a numerical check. We do not have any data for the unfiltered case.
2. If the major contribution to the wall pressure is caused by interaction of the turbulence with the mean shear and if the scale of the covariance \overline{vw} increases when one is farther from the wall the plotted $\overline{p(o)V}$ values would seem to be consistent with our results. Also, the maximum measured value of $\overline{p(o)V}$ in any plane parallel to the wall decreases as one considers planes farther from the wall; they do not increase.
3. We have not measured the term $\overline{p(o)w}$, only $\overline{p(o)V}$ and $\overline{p(o)u}$. The turbulent flow is statistically homogeneous in the z-direction parallel to the surface and normal to the stream. Therefore the correlation $\overline{p(o)w}$ must be zero in a plane normal to the wall containing the free stream velocity and the pressure transducer.

Our measurements of $\overline{p(o)u}$ and $\overline{p(o)V}$ imply that a large part of the wall pressure $\overline{p(o)}$ is produced by interaction of the v velocity of turbulence with the mean stream. I do not believe that our measurements of $\overline{p(o)u}$ and $\overline{p(o)v}$ accurately reflect the role of the turbulent pressure in the turbulent energy transfer. One would expect correlations with w if one could measure the turbulent pressure in the fluid.

J.S. Serafini

Would Dr. Willmarth care to comment on the effect of his having had to filter out the low frequency portion of his spectra before performing the correlation?

Authors' reply

In a Journal of Fluid Mechanics paper on our prior work (Willmarth & Wooldridge, 1962) the disturbances in the wind tunnel were discussed. One type of disturbance that we found consisted of large eddies with axes parallel to the stream and near the wall which produced large wall pressure fluctuations at low frequencies. We were forced to filter our signals and reject the low frequency components. It appears to me that it is possible that you can obtain extraneous pressure velocity correlations from these eddies because they are not stationary but undulate in a random fashion as they pass over the measuring station.

Comment by J.S. Serafini

It should be pointed out that in connection with the comment on the interference of the hot-wire probe on the spectra of the wall-pressure fluctuations, my measurements also show that the probe interference must be taken into account. My comment here is simply the point that in filtering out the interference effect at low frequencies, the filter cannot help but eliminate the low frequency portion of the spectra which ordinarily is unaffected by the interference situation. Consequently, this may appear in the data to approximate the decrease in level with decreasing frequency, i.e. the 'low-frequency drop-off' that Lilley and Hodgson have obtained in their theoretical calculation. Thus, it is readily seen that the caution must be exercised in the interpretation of these filtered results with intention of applying them to the theoretical models which either require or imply the existence of the 'low-frequency drop-off' of the spectra.

Comment by M.K. Bull

In correlation measurements between wall pressure and streamwise velocity component made at the University of Southampton, correlations similar to those shown by Dr. Serafini were found but contained low frequency interference between hot wire probe and pressure transducers. When the interference effects were removed by filtering out frequencies for which $\omega\delta^*/U_0 < 0.15$, curves similar to those shown by Professor Willmarth were obtained.

DISTRIBUTION

Copies of AGARD publications may be obtained in the various countries at the addresses given below.

On peut se procurer des exemplaires des publications de l'AGARD aux adresses suivantes.

BELGIUM BELGIQUE	Centre National d'Etudes et de Recherches Aéronautiques 11, rue d'Egmont, Bruxelles
CANADA	Director of Scientific Information Service Defense Research Board Department of National Defense 'A' Building, Ottawa, Ontario
DENMARK DANEMARK	Military Research Board Defense Staff Kastellet, Copenhagen Ø
FRANCE	O.N.E.R.A. (Direction) 25, Avenue de la Division Leclerc Châtillon-sous-Bagneux (Seine)
GERMANY ALLEMAGNE	Zentralstelle für Luftfahrt- dokumentation und -information München 27, Maria-Theresia Str. 21 Attn: Dr. H.J. Rautenberg
GREECE GRECE	Greek National Defense General Staff B. MEO Athens
ICELAND ISLANDE	Director of Aviation c/o Flugrad Reykjavik
ITALY ITALIE	Ufficio del Generale Ispettore del Genio Aeronautico Ministero Difesa Aeronautica Roma
LUXEMBURG LUXEMBOURG	Obtainable through Belgium
NETHERLANDS PAYS BAS	Netherlands Delegation to AGARD Michiel de Ruyterweg 10 Delft

NORWAY NORVEGE	Mr. O. Blichner Norwegian Defence Research Establishment Kjeller per Lilleström
PORTUGAL	Col. J.A. de Almeida Viama (Delegado Nacional do 'AGARD') Direcção do Serviço de Material da F.A. Rua da Escola Politecnica, 42 Lisboa
TURKEY TURQUIE	Ministry of National Defence Ankara Attn. AGARD National Delegate
UNITED KINGDOM ROYAUME UNI	Ministry of Aviation T.I.L., Room 009A First Avenue House High Holborn London W.C.1
UNITED STATES ETATS UNIS	National Aeronautics and Space Administration (NASA) 1520 H Street, N.W. Washington 25, D.C.



<p>AGARD Report 456 North Atlantic Treaty Organization, Advisory Group for Aeronautical Research and Development MEASUREMENTS OF THE CORRELATION BETWEEN THE FLUCTUATING VELOCITIES AND THE FLUCTUATING WALL PRESSURE IN A THICK TURBULENT BOUNDARY LAYER W.W. Willmarth and C.E. Wooldridge 1963 62 pp., incl. 23 refs., 43 figs., appendix & discussion</p> <p>Turbulent motion in a thick (5 inch) boundary layer with zero longitudinal pressure gradient which is produced by natural transition on a smooth surface has been studied. Measurements have been made of the space-time correlation between the fluctuating</p> <p>P. T. O.</p>	<p>532.526.4 3b2f</p>	<p>AGARD Report 456 North Atlantic Treaty Organization, Advisory Group for Aeronautical Research and Development MEASUREMENTS OF THE CORRELATION BETWEEN THE FLUCTUATING VELOCITIES AND THE FLUCTUATING WALL PRESSURE IN A THICK TURBULENT BOUNDARY LAYER W.W. Willmarth and C.E. Wooldridge 1963 62 pp., incl. 23 refs., 43 figs., appendix & discussion</p> <p>Turbulent motion in a thick (5 inch) boundary layer with zero longitudinal pressure gradient which is produced by natural transition on a smooth surface has been studied. Measurements have been made of the space-time correlation between the fluctuating</p> <p>P. T. O.</p>	<p>532.526.4 3b2f</p>
<p>AGARD Report 456 North Atlantic Treaty Organization, Advisory Group for Aeronautical Research and Development MEASUREMENTS OF THE CORRELATION BETWEEN THE FLUCTUATING VELOCITIES AND THE FLUCTUATING WALL PRESSURE IN A THICK TURBULENT BOUNDARY LAYER W.W. Willmarth and C.E. Wooldridge 1963 62 pp., incl. 23 refs., 43 figs., appendix & discussion</p> <p>Turbulent motion in a thick (5 inch) boundary layer with zero longitudinal pressure gradient which is produced by natural transition on a smooth surface has been studied. Measurements have been made of the space-time correlation between the fluctuating</p> <p>P. T. O.</p>	<p>532.526.4 3b2f</p>	<p>AGARD Report 456 North Atlantic Treaty Organization, Advisory Group for Aeronautical Research and Development MEASUREMENTS OF THE CORRELATION BETWEEN THE FLUCTUATING VELOCITIES AND THE FLUCTUATING WALL PRESSURE IN A THICK TURBULENT BOUNDARY LAYER W.W. Willmarth and C.E. Wooldridge 1963 62 pp., incl. 23 refs., 43 figs., appendix & discussion</p> <p>Turbulent motion in a thick (5 inch) boundary layer with zero longitudinal pressure gradient which is produced by natural transition on a smooth surface has been studied. Measurements have been made of the space-time correlation between the fluctuating</p> <p>P. T. O.</p>	<p>532.526.4 3b2f</p>

wall pressure and the fluctuating velocities in the layer, and between the fluctuating wall pressure and the time derivative of the fluctuating velocity normal to the wall.

This Report is one in the Series 448-469 inclusive, presenting papers, with discussions, given at the AGARD Specialists' Meeting on 'The Mechanism of Noise Generation in Turbulent Flow' at the Training Center for Experimental Aerodynamics, Rhode-Saint-Genèse, Belgium, 1-5 April 1963, sponsored by the AGARD Fluid Dynamics Panel.

wall pressure and the fluctuating velocities in the layer, and between the fluctuating wall pressure and the time derivative of the fluctuating velocity normal to the wall.

This Report is one in the Series 448-469 inclusive, presenting papers, with discussions, given at the AGARD Specialists' Meeting on 'The Mechanism of Noise Generation in Turbulent Flow' at the Training Center for Experimental Aerodynamics, Rhode-Saint-Genèse, Belgium, 1-5 April 1963, sponsored by the AGARD Fluid Dynamics Panel.

wall pressure and the fluctuating velocities in the layer, and between the fluctuating wall pressure and the time derivative of the fluctuating velocity normal to the wall.

This Report is one in the Series 448-469 inclusive, presenting papers, with discussions, given at the AGARD Specialists' Meeting on 'The Mechanism of Noise Generation in Turbulent Flow' at the Training Center for Experimental Aerodynamics, Rhode-Saint-Genèse, Belgium, 1-5 April 1963, sponsored by the AGARD Fluid Dynamics Panel.

wall pressure and the fluctuating velocities in the layer, and between the fluctuating wall pressure and the time derivative of the fluctuating velocity normal to the wall.

This Report is one in the Series 448-469 inclusive, presenting papers, with discussions, given at the AGARD Specialists' Meeting on 'The Mechanism of Noise Generation in Turbulent Flow' at the Training Center for Experimental Aerodynamics, Rhode-Saint-Genèse, Belgium, 1-5 April 1963, sponsored by the AGARD Fluid Dynamics Panel.

<p>AGARD Report 456 North Atlantic Treaty Organization, Advisory Group for Aeronautical Research and Development MEASUREMENTS OF THE CORRELATION BETWEEN THE FLUCTUATING VELOCITIES AND THE FLUCTUATING WALL PRESSURE IN A THICK TURBULENT BOUNDARY LAYER W.W. Willmarth and C.E. Wooldridge 1963 62 pp., incl. 23 refs., 43 figs., appendix & discussion</p> <p>Turbulent motion in a thick (5 inch) boundary layer with zero longitudinal pressure gradient which is produced by natural transition on a smooth surface has been studied. Measurements have been made of the space-time correlation between the fluctuating</p> <p>P. T. O.</p>	<p>532.526.4 3b2f</p>	<p>AGARD Report 456 North Atlantic Treaty Organization, Advisory Group for Aeronautical Research and Development MEASUREMENTS OF THE CORRELATION BETWEEN THE FLUCTUATING VELOCITIES AND THE FLUCTUATING WALL PRESSURE IN A THICK TURBULENT BOUNDARY LAYER W.W. Willmarth and C.E. Wooldridge 1963 62 pp., incl. 23 refs., 43 figs., appendix & discussion.</p> <p>Turbulent motion in a thick (5 inch) boundary layer with zero longitudinal pressure gradient which is produced by natural transition on a smooth surface has been studied. Measurements have been made of the space-time correlation between the fluctuating</p> <p>P. T. O.</p>	<p>532.526.4 3b2f</p>
<p>AGARD Report 456 North Atlantic Treaty Organization, Advisory Group for Aeronautical Research and Development MEASUREMENTS OF THE CORRELATION BETWEEN THE FLUCTUATING VELOCITIES AND THE FLUCTUATING WALL PRESSURE IN A THICK TURBULENT BOUNDARY LAYER W.W. Willmarth and C.E. Wooldridge 1963 62 pp., incl. 23 refs., 43 figs., appendix & discussion.</p> <p>Turbulent motion in a thick (5 inch) boundary layer with zero longitudinal pressure gradient which is produced by natural transition on a smooth surface has been studied. Measurements have been made of the space-time correlation between the fluctuating</p> <p>P. T. O.</p>	<p>532.526.4 3b2f</p>	<p>AGARD Report 456 North Atlantic Treaty Organization, Advisory Group for Aeronautical Research and Development MEASUREMENTS OF THE CORRELATION BETWEEN THE FLUCTUATING VELOCITIES AND THE FLUCTUATING WALL PRESSURE IN A THICK TURBULENT BOUNDARY LAYER W.W. Willmarth and C.E. Wooldridge 1963 62 pp., incl. 23 refs., 43 figs., appendix & discussion.</p> <p>Turbulent motion in a thick (5 inch) boundary layer with zero longitudinal pressure gradient which is produced by natural transition on a smooth surface has been studied. Measurements have been made of the space-time correlation between the fluctuating</p> <p>P. T. O.</p>	<p>532.526.4 3b2f</p>

wall pressure and the fluctuating velocities in the layer, and between the fluctuating wall pressure and the time derivative of the fluctuating velocity normal to the wall.

This Report is one in the Series 448-469 inclusive, presenting papers, with discussions, given at the AGARD Specialists' Meeting on 'The Mechanism of Noise Generation in Turbulent Flow' at the Training Center for Experimental Aerodynamics, Rhode-Saint-Genèse, Belgium, 1-5 April 1963, sponsored by the AGARD Fluid Dynamics Panel.

wall pressure and the fluctuating velocities in the layer, and between the fluctuating wall pressure and the time derivative of the fluctuating velocity normal to the wall.

This Report is one in the Series 448-469 inclusive, presenting papers, with discussions, given at the AGARD Specialists' Meeting on 'The Mechanism of Noise Generation in Turbulent Flow' at the Training Center for Experimental Aerodynamics, Rhode-Saint-Genèse, Belgium, 1-5 April 1963, sponsored by the AGARD Fluid Dynamics Panel.

wall pressure and the fluctuating velocities in the layer, and between the fluctuating wall pressure and the time derivative of the fluctuating velocity normal to the wall.

This Report is one in the Series 448-469 inclusive, presenting papers, with discussions, given at the AGARD Specialists' Meeting on 'The Mechanism of Noise Generation in Turbulent Flow' at the Training Center for Experimental Aerodynamics, Rhode-Saint-Genèse, Belgium, 1-5 April 1963, sponsored by the AGARD Fluid Dynamics Panel.

wall pressure and the fluctuating velocities in the layer, and between the fluctuating wall pressure and the time derivative of the fluctuating velocity normal to the wall.

This Report is one in the Series 448-469 inclusive, presenting papers, with discussions, given at the AGARD Specialists' Meeting on 'The Mechanism of Noise Generation in Turbulent Flow' at the Training Center for Experimental Aerodynamics, Rhode-Saint-Genèse, Belgium, 1-5 April 1963, sponsored by the AGARD Fluid Dynamics Panel.

UNCLASSIFIED

UNCLASSIFIED